JOURNAL OF BACTERIOLOGY, June 2008, p. 4001–4016 Vol. 190, No. 11
0021-9193/08/$08.00+0 doi:10.1128/JB.00135-08

Insight from TonB Hybrid Proteins into the Mechanism of Iron Transport through the Outer Membrane▽

Wallace A. Kaserer, Xiaoxu Jiang, Qiaobin Xiao, Daniel C. Scott, Matthew Bauler, Daniel Copeland, Salete M. C. Newton, and Phillip E. Klebba*

Department of Chemistry and Biochemistry, University of Oklahoma, 620 Parrington Oval, Norman, Oklahoma 73019

Received 25 January 2008/Accepted 24 March 2008

We created hybrid proteins to study the functions of TonB. We first fused the portion of *Escherichia coli tonB* that encodes the C-terminal 69 amino acids (amino acids 170 to 239) of TonB downstream from *E. coli malE* (MalE-TonB69C). Production of MalE-TonB69C in *tonB*$^+$ bacteria inhibited siderophore transport. After overexpression and purification of the fusion protein on an amylose column, we proteolytically released the TonB C terminus and characterized it. Fluorescence spectra positioned its sole tryptophan (W213) in a weakly polar site in the protein interior, shielded from quenchers. Affinity chromatography showed the binding of the TonB C-domain to other proteins: immobilized TonB-dependent (FepA and colicin B) and TonB-independent (FepAΔ3-17, OmpA, and lysozyme) proteins adsorbed MalE-TonB69C, revealing a general affinity of the C terminus for other proteins. Additional constructions fused full-length TonB upstream or downstream of green fluorescent protein (GFP). TonB-GFP constructs had partial functionality but no fluorescence; GFP-TonB fusion proteins were functional and fluorescent. The activity of the latter constructs, which localized GFP in the cytoplasm and TonB in the cell envelope, indicate that the TonB N terminus remains in the inner membrane during its biological function. Finally, sequence analyses revealed homology in the TonB C terminus to *E. coli* YcfS, a proline-rich protein that contains the lysin (LysM) peptidoglycan-binding motif. LysM structural mimicry occurs in two positions of the dimeric TonB C-domain, and experiments confirmed that it physically binds to the murein sacculus. Together, these findings infer that the TonB N terminus remains associated with the inner membrane, while the downstream region bridges the cell envelope from the affinity of the C terminus for peptidoglycan. This architecture suggests a membrane surveillance model of action, in which TonB finds occupied receptor proteins by surveying the underside of peptidoglycan-associated outer membrane proteins.

Iron is one target of gram-negative bacterial cell envelope transport systems, and microbes elaborate high-affinity siderophores that complex extracellular iron (70). However, ferric siderophores, like ferric enterobactin (FeEnt), are too large (716 Da) to pass through general porins in the outer membrane (OM), necessitating a different type of transporter to acquire them. On the basis of their 22-stranded transmembrane β-barrels, OM metal transporters like FepA belong to the porin superfamily (89). Ligand binding to such receptors initiates the transport reaction through their transmembrane channels, which led to their designation as ligand-gated porins (LGP) (88), by analogy to the family of eukaryotic ligand-gated ion channels. It is noteworthy that LGP are mechanistically distinct from general, diffusive porins because they bind metal complexes with high affinity and actively transport them against a concentration gradient into the cell. Once in the periplasm, binding proteins adsorb ferric siderophores and deliver them to inner membrane (IM) permeases that actively transport either the metal complex or free iron into the cytoplasm. At the binding stage of the uptake process, ferric siderophores compete with noxious agents like bacteriophages (H8 [85a] and T5 and ϕ80 [18, 103]) and colicins (B, D [37], and M [18]) for entry into the cell. OM transport of metal complexes and susceptibility to phages and colicins require metabolic energy (13, 25, 85) and usually involve participation of an additional cell envelope protein, TonB.

Bioinformatic and biophysical data suggest that TonB comprises three parts that reside in different regions of the cell envelope: a hydrophobic N-terminal sequence in the IM (27), a central section that spans the periplasm (30, 39), and a C-terminal ββαβ domain, also in the periplasm, that peripherally associates with the OM (26, 52, 76, 78, 95). Sequence analyses suggested that the upstream, N-terminal portion of TonB contains one or more membrane-embedded regions (49), including a hydrophobic helix that anchors the protein in the IM. Gene fusion experiments supported this notion (86), but no structural data are available on the N terminus. Nuclear magnetic resonance data on synthetic peptides suggested that multiply repeated Glu-Pro and Lys-Pro sequences in the central portion behave like two long rods, joined by a short sequence with some flexibility, that span over 100 Å (20, 30). The C terminus of TonB, which is important to its function (4), forms a ββαβ motif that may dimerize (26, 52) and recruit other polypeptides into its β-sheet (76, 95). There is evidence that TonB dimerizes in vivo (90), but whether the dimer is its normal state or whether TonB fluctuates between monomeric and dimeric forms in vivo is not known. The physiology and biochemistry of TonB action remain obscure, but recent data confirm the idea (36, 46) that TonB binds to sites on the periplasmic surface of TonB-dependent OM proteins. This protein-protein interaction may facilitate LGP transport.

* Corresponding author. Mailing address: Department of Chemistry and Biochemistry, University of Oklahoma, 620 Parrington Oval, Norman, OK 73019. Phone: (405) 325-4969. Fax: (405) 325-6111. E-mail: peklebba@ou.edu.

▽ Published ahead of print on 4 April 2008.

TABLE 1. Bacterial strains and plasmids

Strain or plasmid	Relevant genotype or gene[a]	Source or reference
E. coli strains		
BN1071	*entA fepA*$^+$ *tonB*$^+$ *rpsL*	48
KDO23	BN1071 *tonB*	This study
OKN1	BN1071 Δ*tonB*	60
OKN3	BN1071 Δ*fepA*	60
ER2507	(*malB*) *zjb*::Tn*5 rpsL supE44 fhuA*	New England Biolabs
BL21(DE3)	λ lysogen, *lon ompT*	Novagen
Plasmids		
pRZ540	*tonB*$^+$ (TonB)	81
pMalp2	*malE* fusion vector (MalE)	New England Biolabs
pSTonB239	pMalp2 *malE-tonB*$_{1\text{-}239}$ (MalE-TonB)	This study
pSTonB135C	pMalp2 *malE-tonB*$_{104\text{-}239}$ (MalE-TonB135C)	This study
pSTonB69C	pMalp2 *malE-tonB*$_{100\text{-}239}$ (MalE-TonB69C)	This study
pHSG575	Low-copy-number cloning vector	40
pT23	pHSG575 *tonB*$^+$ (TonB)	This study
pTG	pHSG575 *tonB-ssgfp* (TonB-GFP)	This study
pTatTG	pHSG575 *tatss-tonB-ssgfp* (TatTonB-GFP)	This study
pΔssTG	pHSG575 *tonB 4-32-ssgfp* (4-32TonB-GFP)	This study
pTpG	pHSG575 *tonB* promoter-*ssgfp* (GFP)	
pGT	pHSG575 *tonB* promoter-*ssgfp-tonB* (GFP-TonB)	This study
pGLT	pHSG575 *tonB* promoter-*ssgfp-tonB* (GFP-L-TonB)	This study
pGTΔ69C	pHSG575 *tonB* promoter-*ssgfp-ton*B$_{170\text{-}239}$ (GFP-TonB69C)	This study
pCol1	pUC18 *cba cbi* (colicin B)	This study
pETTonB	pET28 *6H-tonB* (6H-TonB)	This study

[a] For plasmids, the expressed protein is shown in parentheses.

We biochemically characterized TonB hybrid proteins and its isolated C-terminal domain to gain insight into the functions of TonB in OM iron transport. Overexpression of the fusion polypeptides in a *tonB*$^+$ background inhibited siderophore uptake, but not colicin susceptibility. The C-terminal polypeptide adsorbed to FepA-agarose and also to OmpA-agarose and to agarose bearing FepAΔ13-22, which lacks the TonB box. Thus, the TonB C terminus showed a general affinity for OM proteins that does not involve interactions with the TonB box sequence. Green fluorescent protein (GFP)-TonB hybrid proteins were fluorescent and functional in TonB-dependent processes, refuting the idea that the TonB N terminus leaves the IM during performance of its biochemical activity (55, 57). Last, the C terminus of TonB contains previously unrecognized regions that are structurally related to the lysin (LysM) domain (7) that confers peptidoglycan (PG) binding to *Escherichia coli* YcfS and its homologs.

MATERIALS AND METHODS

Bacterial strains and plasmids. Most strains (Table 1) originated from *E. coli* BN1071 (F$^-$ *entA pro trpB1*) (48), including KDO23 (*entA tonB*), a spontaneous *tonB* mutant from simultaneous selection against colicins B, M, and I$_a$, and OKN1 (Δ*tonB*) (60), which contains a genetically engineered, precise deletion of the structural gene. Our motivation for constructing the latter strain was that chromosomal fragments of siderophore receptor genes may unexpectedly complement exogenous genes on plasmids (101). To avoid such phenomena in the *tonB* background, we completely deleted (28) *tonB* and then used the strain as a host for plasmids bearing *tonB*$^+$ or its derivatives. After isolation of strains KDO23 and OKN1, we screened them for susceptibility to colicins and ability to transport ferric siderophores; we confirmed their mutations by PCR analysis. In addition, we performed Western immunoblotting with polyclonal rabbit anti-TonB sera and monoclonal mouse anti-FepA sera to verify the absence of TonB and presence of FepA. In both strains, the *tonB*$^+$ phenotype was reinstated, as evidenced by colicin sensitivity and siderophore nutrition, upon transformation with pRZ540 (*tonB*$^+$) (81). Strain ER2507 (*malE*; New England Biolabs) was the host strain for pMal fusion plasmids.

pMalp2 (New England Biolabs) (29) contains a P$_{tac}$ promoter that regulates transcription of its MalE-LacZ fusion. Using the multiple cloning site of this vector, we replaced the *lacZ* moiety with other genes or gene fragments of interest. We amplified the DNA encoding the 69 C-terminal residues of *E. coli tonB* from pRZ540 (81, 83), purified the 500-bp product from agarose with Geneclean (Bio 101, Vista, CA), and digested it with XmnI and HindIII. The PCR band was ligated into pMalp2, and the resulting transformant clones were screened by restriction analysis with EcoRV and HindIII. Candidate plasmids with the appropriately sized restriction fragment were sequenced with an ALF-Express automated DNA sequencer (Pharmacia). We designated the product pSTonB69C; similarly constructed variants that fused the region that encodes the C-terminal 135 residues or the intact *tonB* gene to MalE were pSTonB135C and pSTonB239, respectively. We regulated expression of the fusion proteins by varying the isopropyl-β-D-thiogalactopyranoside (IPTG) concentration in culture media and purified the resulting hybrid proteins by affinity chromatography on amylose resin (32).

We also fused the structural gene for GFP to *tonB* in several ways. pT23, a derivative of the low-copy vector pHSG575, carries a wild-type chromosomal *tonB* structural gene (from *E. coli* BN1071) under control of its natural promoter. pQbioT7-GFP (QbioGene, Irvine, CA) carries a mutant version of the *Aequorea victoria* GFP structural gene (*sggfp*) that contains the substitutions F64L, S65C, and I167T. The first mutation confers greater solubility, stability, and fluorophore formation at 37°C, whereas the latter two optimize the protein's single excitation peak at 474 nm. Using PCR, we separately amplified the *E. coli tonB* promoter region and the *tonB* structural gene from pT23 and the *sggfp* gene from pQbioT7-GFP. We first fused *ssgfp* in frame with and downstream from *tonB* on pT23 (pTG and derivatives). Second, we cloned *ssgfp* (with its stop codon) immediately downstream from the *tonB* promoter (pTpG), and in another clone, we introduced *ssgfp* (without a stop codon) in frame between the *tonB* promoter and the *tonB* structural gene (pGT). In the latter case, primers introduced HindIII and XbaI cleavage sites at the 5′ and 3′ ends, respectively, of the *tonB* promoter region, XbaI and BamHI sites at the 5′ and 3′ ends, respectively, of *sggfp*, and BamHI and EcoRI sites at the 5′ and 3′ ends of *tonB*. After digestion with the appropriate restriction enzymes, we joined the three fragments with T4 ligase to produce *tonB* promoter-*sggfp-tonB*. The final 2,117-bp product and pHSG575 were digested with HindIII and EcoRI, agarose purified, and joined with T4 ligase to produce pGT. In pGLT, the 5-amino-acid linker sequence EAAAK was inserted between GFP and TonB by QuikChange mutagenesis at the 5′ end of the *tonB* moiety in pGT. The result altered the N-terminal sequence

of TonB from MTLDLPRR to MAEAAAKA. This construct is predicted (5) to form a small helical peptide between GFP and TonB.

Isolation of the TonB C terminus. *E. coli* ER2507/pSTonB69C was grown overnight in LB broth (68) with ampicillin and streptomycin at 100 μg/ml and subcultured at 1% into LB broth containing 0.2% glucose. When the culture reached an optical density at 600 nm of 0.5, we added 0.5 mM IPTG to the culture; after the culture was subjected to shaking for 3 h at 37°C, we collected the cells by centrifugation at 3,000 × *g* for 20 min and resuspended them in buffer A (10 mM Tris-HCl, 0.4 M NaCl, 1 mM EDTA, and 10 mM β-mercaptoethanol). After lysis by passage through a French pressure cell (three times at 14,000 lb/in^2), we clarified the lysate by ultracentrifugation at 100,000 × *g* for 30 min and chromatographed the supernatant on an amylose column (approximately 15 ml) equilibrated with buffer A (32). After the column was washed with 10 bed volumes of buffer A, we eluted adsorbed proteins with 10 mM maltose in buffer A. The eluted fractions were pooled and dialyzed against Tris-buffered saline (TBS) (50 mM Tris chloride [pH 7.5] and 0.5 M NaCl), sodium dodecyl sulfate (SDS) was added to 0.05%, and TonB69C was cleaved by digestion with factor Xa. The digestion products were resolved on Sephacryl S100HR (Pharmacia) in TBS plus 0.05% SDS, and the SDS was removed from pooled fractions of TonB69C by acetone precipitation.

Fractionation of cell envelopes. Bacteria were cultured in L broth (67), subcultured in morpholinepropanesulfonic acid (MOPS) minimal medium (69), harvested in mid-exponential phase of growth, washed with and resuspended in TBS, and chilled on ice. OM and IM fragments were formed by lysis of bacteria in a French pressure cell (96) and purified by sucrose gradient centrifugation (72).

Proteins and antisera. Hen egg white lysozyme was purchased from Sigma. *E. coli* OM proteins OmpA, FepA, and FepAΔ13-17 were purified by differential extraction of cell envelopes with Triton X-100 (77, 91). Colicin B (ColB) was derived from supernatants of *E. coli* DM1187/pCol1, and factor X was from bovine blood; we purified both the toxin (77) and the protease (105) by conventional chromatographic methods and activated factor X to factor Xa with snake venom (45). *E. coli* MalE was purified from *E. coli* ER2507/pMalp2 after IPTG induction by French pressure cell lysis and subsequent amylose chromatography (32). *E. coli* FepB was purified as previously described (97). Colicin titer was expressed as the reciprocal of the highest dilution that resulted in a clearing of a lawn of a sensitive bacterial strain.

Full-length TonB was purified as a His-tagged soluble protein. The *tonB* structural gene on pRZ540 was amplified by PCR and cloned in pET28 (EMD Biosciences) to create an N-terminal six-histidine tag. The resulting plasmid (pETTonB) was transformed into *E. coli* BL21(DE3) (Invitrogen) and induced to high levels of 6H-TonB synthesis by growth in LB broth with IPTG (0.5 mM). 6H-TonB was purified in a single step by passage of crude cell lysates over Ni^{2+}-nitrilotriacetic acid agarose (Qiagen). Rabbits were intramuscularly immunized with purified 6H-TonB (50 to 100 μg) six times over a 6-week period, with Freund's complete adjuvant in the first injection and with Freund's incomplete adjuvant or alum in subsequent injections. Rabbits were bled by cardiac puncture, and anti-TonB sera was prepared and diluted 10^5-fold for use in Western immunoblots.

Electrophoresis and Western immunoblots. For SDS-polyacrylamide gel electrophoresis (PAGE) (60), samples were suspended in SDS sample buffer plus 3% β-mercaptoethanol, heated at 100°C for 5 min, and electrophoresed on 10% polyacrylamide slabs. For Western immunoblots, proteins were transferred to nitrocellulose paper, blocked in TBS plus 1% gelatin, and incubated with murine ascitic fluid (0.5%) or polyclonal rabbit antisera (0.01%) in TBS plus 1% gelatin for 3 h. The nitrocellulose paper was washed in TBS plus 0.05% Tween 20, incubated with alkaline phosphatase-conjugated goat anti-mouse immunoglobulin or alkaline phosphatase-conjugated goat anti-rabbit immunoglobulin, respectively, for 2 h, washed, and developed with bromochloroindolyl phosphate and nitroblue tetrazolium (88).

Conjugation of proteins to Sepharose 6B. Aliquots (25 ml) of Sepharose 6B were activated by the dropwise addition of 6 g CNBr in distilled water, while maintaining the pH between 11.0 and 12.0 (62). The resin was washed with distilled water and suspended in the appropriate conjugation buffer. For OM proteins, 50 mg of purified material was dissolved in 0.2 M $NaHCO_3$ containing 2% Triton X-100, added to the activated resin, and incubated overnight at 4°C with gentle stirring (6, 74, 80). After conjugation, the resin was washed with 2 liters of distilled water, 2 liters of 1 M acetic acid, and 2 liters of distilled water. Aliquots of the first wash were saved to determine the efficiency of protein conjugation, which was usually >95%. For non-OM proteins, Triton X-100 was omitted from the conjugation buffer. After modification, we equilibrated the resins in TBS, pH 7.5.

Spectroscopic measurements. UV-visible spectra were acquired on a Beckman DU 640 spectrophotometer in 1.0-cm cuvettes. Circular dichroism (CD) spectra were obtained using an AVIV 60DS CD spectrometer. Either 0.1- or 1.0-cm cuvettes were used to measure the CD spectra of TonB6C9. For fluorescence spectroscopy, excitation and emission spectra were recorded with an SLM8000 fluorimeter upgraded to 8100 functionality (SLM Instruments, Rochester, NY), equipped with a 450-watt xenon light source and a cooled photomultipler tube housing, operated in the photon-counting mode.

Sequence and structural analyses. Protein sequences were obtained from NCBI and initially studied by BLASTP to identify their homologous relatives in the NCBI database. Orthologs and paralogs were then compared by CLUSTALW to discern regions of identity and similarity. When crystallographic data were available, related polypeptides and structural motifs were aligned and superimposed by LSQMAN (50, 53). The overlay was performed using 1IHR, the 1.55-Å structure of the dimeric TonB C terminus, and the first model in 1E0G, the LysM domain from *E. coli* MltD. The first model was chosen because the PDB file gave no information on the best representative conformer in the ensemble. LSQMAN used brute-force alignment, with a search fragment length of 5 amino acids and a step size of 2, searching for the maximum number of matched residues. The program produced graphic output of the structural relationships.

PG binding experiments. PG was purified from exponential-phase *E. coli* BN1071 by standard procedures (34, 35, 64). Bacteria from 500 ml of LB broth, growing exponentially with aeration (to an optical density at 600 nm of ~0.7 to 0.9), were rapidly chilled in an ice-salt-water bath, harvested by centrifugation at 4°C, and resuspended in 5 ml of ice-cold water. The cell suspension was added dropwise to 10 ml of boiling 4% SDS solution in a 50-ml Erlenmeyer flask on a hot plate over a period of about 10 min. After the solution was boiled for 30 min, it was allowed to cool to room temperature and stand overnight. The crude sacculi were collected by ultracentrifugation (100,000 × *g*, 1.5 h) and washed free of SDS by repeated resuspensions in 15 ml of water and ultracentrifugations (four times). α-Amylase (100 μg/ml in 10 mM Tris-HCl [pH 7.0]) was added and incubated for 2 h at 37°C to degrade high-molecular-weight glycogen; pronase (preincubated at 60°C for 2 h to inactivate any contaminating lysozyme) was added (200 μg/ml) and incubated for 2 h at 37°C to digest bound lipoprotein and any other protein contaminations. SDS was added to a concentration of 1%, and the sacculi were boiled for 15 min. The SDS was removed by repeated centrifugations and resuspensions in water (four times). The purified sacculi were stored in water containing 0.05% sodium azide at 4°C at a concentration of about 1 mg/ml.

For binding studies, aliquots of purified PG were mixed with 30-μg aliquots of purified proteins (MalE, MalE-TonB69C, and FepB) in 20 mM Tris-Cl, pH 8 (final volume of 100 μl) at room temperature for 30 min and then centrifuged at 100,000 × *g* for 45 min in a Beckman Optima TL ultracentrifuge. Both the supernatants and the resuspended pellets were subjected to SDS-PAGE. The gels were stained with Coomassie blue, photographed, and analyzed by ImageQuant (Molecular Dynamics) to determine the amount of protein in the pellets and supernatants.

RESULTS

Cloning, expression, and purification of TonB69C. We genetically fused DNA encoding the C-terminal 69 residues of TonB (amino acids 170 to 239) downstream from *malE* on pMalp2 and purified the resulting hybrid protein (MalE-TonB69C) by affinity chromatography on an amylose resin (29, 32, 100). The electrophoretic mobility of MalE-TonB69C on SDS-polyacrylamide gels was slightly less than that expected for a protein of its predicted size, 49.5 kDa (Fig. 1A). However, TonB itself has aberrant, decreased mobility on SDS-polyacrylamide gels. After IPTG induction to high levels of expression, we isolated the fusion protein in high yield (50 mg/liter of culture media) and 95% homogeneity (Fig. 1).

MalE-TonB69C contains a factor Xa cleavage site between the two polypeptides, but it was susceptible to the protease only in the presence of 0.05% SDS, suggesting that in the native state the cleavage site is buried in protein structure. The factor Xa digestion products were resolved on a Sephacryl S100HR gel filtration column in TBS containing 0.05% SDS,

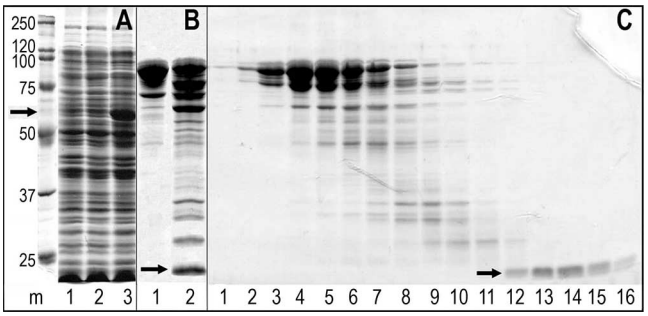

FIG. 1. Expression and purification of MalE-TonB69C. *E. coli* KDO23/pSTonB69C was grown to mid-log in LB broth, IPTG was added to 0.5 mM, and the cells were shaken at 37°C for 3 more hours. (A) Aliquots of 10^8 cells were collected before (lane 1) and 1 h (lane 2) and 2 hours (lane 3) after the addition of IPTG. The bacteria were lysed and subjected to SDS-PAGE on a 10% gel. The overexpression of MalE-TonB69C (arrow) appears in lane 3. The positions of molecular size markers (m) (in kilodaltons), Bio-Rad Precision Plus protein standards, are shown to the left of the gel. (B) After lysis by passage through a French pressure cell, the lysate was clarified by centrifugation at 100,000 × *g* for 30 min and applied to an amylose column. MalE-TonB69C was eluted with maltose (lane 1), and TonB69C (arrow) was released by digestion with factor X_a (lane 2) (16% gel). (C) The digestion mixture was chromatographed on Sephacryl S-100 in TBS plus 0.05% SDS and analyzed on a 16% gel. The arrow indicates the position of TonB69C, which eluted last from the column (lanes 12 to 16).

resulting in >95% purity of the 8-kDa TonB69C polypeptide (Fig. 1). Purified TonB69C was concentrated by acetone precipitation and suspended in 20 mM Tris-Cl, pH 7.5.

Spectroscopic characterizations. The C terminus of TonB contains a single tryptophan residue at position 213 within the α-helix of the domain. Measurements of its intrinsic fluorescence revealed a maximum at 338 nm (Fig. 2). Stepwise additions of the denaturant guanidinium hydrochloride (ultimately to 4 M) sequentially shifted the emission maximum to 352 nm and decreased fluorescence intensity 45%. The emission maximum of the denatured polypeptide was similar to that of free tryptophan in aqueous solution. These data portrayed the solution structure of TonB69C as consistent with the crystal structure (26) folded into a form that ensconces W213 in an internal, slightly polar environment. CD spectra (Fig. 2) were less informative but showed that the domain contains secondary structure and a defined three-dimensional structure. The presence of significant near-UV signals indicated that TonB69C folded into a well-defined structure with α-helical content and other secondary structure typical of an alpha-beta protein.

Effects of quenchers. We evaluated the susceptibility of W213 to quenching by acrylamide, iodide, and cesium. Stern-Volmer analysis of fluorescence in the presence of acrylamide yielded Stern-Volmer constants (K_{sv}s) of 5.9 ± 0.4 for native TonB69C and 8.4 ± 0.4 for denatured TonB69C (Fig. 2). The charged species iodide and cesium less effectively quenched W213 fluorescence: the K_{sv} values were 2.6 ± 0.2 and 4.4 ± 0.1 when the native and denatured polypeptides, respectively, were exposed to iodide, and 0.37 ± 0.005 and 1.6 ± 0.001, respectively, when they were exposed to cesium. Increased ionic strength (0.4 M NaCl) did not perturb the fluorescence emission spectrum (data not shown). The overall linearity of

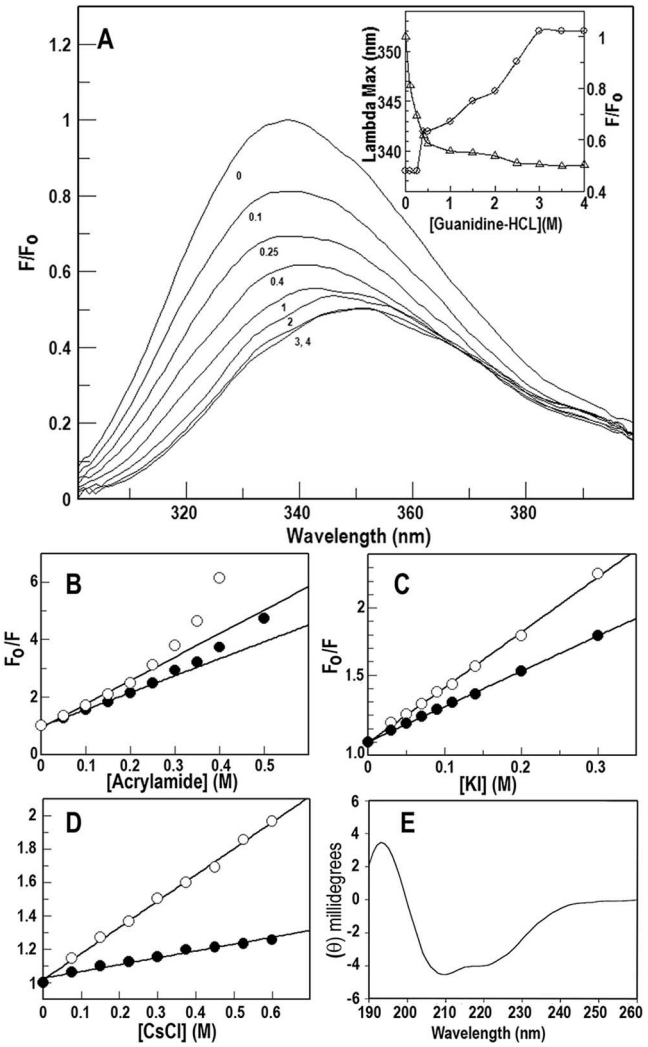

FIG. 2. Spectroscopic properties of TonB69C. (A) Guanidine HCl titration. Fluorescence emission spectra of a single tryptophan (W213) was monitored in the presence of the denaturant guanidine hydrochloride. The red shift of its emission maximum and decrease in fluorescence with increasing concentrations of guanidinium infer the unfolding of the domain and the increasing exposure of the residue to the solvent. The inset plots show emission maximum (E_{max}) (○) and F/F_0 (△) versus the concentration of guanidinium-HCl. (B to D) Susceptibility of TonB69C to quenching. Purified TonB69C, either native (●) or denatured (○), was incubated with increasing concentrations of acrylamide (B), KI (C), and CsCl (D), and its fluorescence emissions were recorded and then analyzed by the Stern-Volmer equation, assuming collisional quenching by the following equation: $F_o/F = 1 + K_{sv}[Q]$, where F_o and F are the fluorescence intensities in the absence or presence, respectively, of the quencher, K_{sv} is the Stern-Volmer constant, and $[Q]$ is the concentration of the quencher. The data were analyzed by linear regression to determine K_{sv} values for each quencher (see the text). (E) Circular dichroism. The CD spectrum of purified TonB69C was recorded in TBS and showed extrema characteristic of α-helical content at 209 nm and other secondary structure at higher wavelengths. The CD data excluded the possibility that TonB69C exists in solution as a random coil form and were consistent with the form of a folded alpha-beta protein.

the Stern-Volmer plots from iodide and cesium (Fig. 2) indicated collisional quenching of W213 in both native and denatured TonB69C. For acrylamide, the Stern-Volmer plots were linear to 0.3 M but deviated from linearity at higher concen-

TABLE 2. Functional analysis of MalE-TonB69C

Strain/plasmid[a]	IPTG concn (mM)	Nutrition test result[b]		ColB[c]
		FeEnt	Fc	
BN1071	0	16	14	5
	1.0	16	14	5
BN1071/pRZ540	0	16	13	5
	1.0	16	13	5
BN1071/pMalp-2	0	16	14	5
	1.0	15.5	14	5
BN1071/pSTonB69C	0	14	14	5
	0.002	14	ND	ND
	0.2	14[d]	0	5
	1.0	0	0	5
KDO23	0	0	0	0
KDO23/pRZ540	0	15	13	5
KDO23/pMal-p2	0	0	0	0
KDO23/pSTonBC69	0	0	0	0
KDO23/pSTonBC69	1.0	0	0	0

[a] The relevant genes of strains and plasmids are as follows: BN1071 (*fepA*$^+$ *tonB*$^+$); KDO23 (*fepA*$^+$ *tonB*); pRZ540 (*tonB*$^+$), pMal-p2 (vector), pSTonB69C (*malE-tonB69C*).

[b] Nutrition test results for FeEnt (3) and ferrichrome (Fc) (71) are expressed as the diameter of the growth halo around the disk (in millimeters). ND, not determined.

[c] Tabulated data indicate the log of the highest dilution that resulted in clearing of a bacterial lawn. ND, not determined.

[d] Faint growth halo.

trations. Again, the data inferred that W213 inhabits an environment of TonB69C where it is more susceptible to the hydrophobic quencher acrylamide and partially shielded from the hydrated charged species iodide and cesium.

Functionality of the isolated TonB C terminus. In agreement with previous reports (90, 93), in *tonB* strains, overexpression of MalE-TonB69C did not restore TonB-dependent processes (Table 2), suggesting that for activity the TonB C terminus must remain connected to the N-terminal domain, presumably anchored in the IM (see below). Overexpression of MalE-TonB69C in wild-type strains inhibited the transport of both FeEnt and ferrichrome (Table 2). The plasmid-derived C-terminal fragment competed with native TonB in a way that impaired the overall ferric siderophore uptake reaction. However, sensitivity to the TonB-dependent colicin B was unaffected by overexpression of MalE-TonB69C. The general permeability of the OM was not compromised by MalE-TonB69C, as shown by the identical antibiotic sensitivity (to chloramphenicol, erythromycin, rifampin, bacitracin, tetracycline, novobiocin, and neomycin [88]) of strains expressing wild-type TonB or its MalE fusion proteins (data not shown).

Adsorption of MalE-TonB69C to proteins. We immobilized FepA, FepAΔ13-17 (which lacks the TonB box), colicin B, OmpA, or lysozyme on cyanogen bromide-activated Sepharose and chromatographed MalE-TonB69C on the derivatized agaroses. We equilibrated the resins in TBS, passed purified fractions of MalE-TonB69C over columns containing the resins, and analyzed the effluents from a salt gradient (0 to 0.5 M NaCl) by immunoblotting with mouse monoclonal anti-MalE (Fig. 3). Neither purified MalE nor MalE-TonB-69C bound to the unconjugated agarose, and MalE alone also passed through resins containing immobilized proteins. Conversely, MalE-TonB69C adsorbed to the protein-modified agaroses and remained bound until it was eluted by the salt gradient. The adsorption of MalE-TonB69C, but not MalE, to the resins indicated that the TonB C terminus was responsible for the binding activity. The relative elution position of MalE-TonB69C in the course of the salt gradient (Fig. 3) suggested the order of its affinity for the conjugated proteins: lysozyme < ColB < OmpA < FepAΔ12-17 < FepA. That is, the least affinity was for lysozyme-Sepharose (MalE-TonB69C eluted earliest in the salt gradient), and the highest affinity was for FepA-Sepharose (MalE-TonB69C eluted last in the salt gradient). The association of TonB69C with FepAΔ13-17 indicated that the interaction did not require binding to the receptor's TonB box. Adsorption to immobilized OmpA and lysozyme demonstrated that the TonB C terminus has general affinity for other proteins. TonB69C had higher affinity for OM proteins, because it required higher salt concentrations to elute from OmpA-Sepharose than from lysozyme-Sepharose: about 50% of the applied MalE-TonB69C passed unabsorbed through the lysozyme-Sepharose column.

TonB-GFP fusions. The paucity of information about the disposition of TonB in vivo led us to explore its localization and function with fusions to the GFP of *Aequorea victoria*. We genetically engineered chimeras that joined the *sggfp* structural gene in frame with and downstream from wild-type *E. coli tonB* on the low-copy plasmid pHSG575, creating pTG (Fig. 4). The construct showed weak TonB activity, as assayed by its ability to facilitate ferric siderophore uptake and colicin sensitivity, but it was not fluorescent. We attempted to convert the TonB-GFP hybrid protein to a fluorescent form by (i) deleting residues in its N-terminal sequence region (amino acids 4 to 32) and (ii) introducing a signal sequence homologous to the TAT consensus signal sequence (Fig. 4). We expected the former construct to localize to the cytoplasm and the latter to enter the cell envelope by the TAT secretion pathway. Immunoblots showed that all the TonB-GFP hybrid proteins were expressed at normal levels (data not shown), but the genetic alterations did not increase the low level of TonB function nor convert their GFP moiety to fluorescence.

We next engineered plasmids that inserted the *sggfp* structural gene downstream from the native *tonB* promoter (pTpG; encodes GFP under the Fur-regulated TonB promoter) or in frame between the *tonB* promoter and the *tonB* structural gene on pHSG575 (pGT and pGLT; Fig. 4). The hybrid proteins encoded by pGT (GFP-TonB) and pGLT (GFP-L-TonB) were identical except that the latter contained the 5-amino-acid linker sequence EAAAK between GFP and TonB. When the hybrid proteins were expressed in strain OKN1 or BN1071, they were both fluorescent, and microscopy revealed that the fluorescence was associated with the cell envelope, rather than distributed in the cytoplasm, as it was for cytoplasmic GFP alone (pTpG) (Fig. 5A). Cell envelope fractionation of cells expressing GFP-TonB and GFP-L-TonB confirmed that both fusion proteins partitioned in the IM and OM, as did wild-type TonB (57) (Fig. 5). It was significant that whether wild-type TonB was expressed from the chromosome or from plasmid pHSG575, it preferentially associated with the OM (Fig. 5E). Cell lysis and cell envelope fractionation resulted in partial

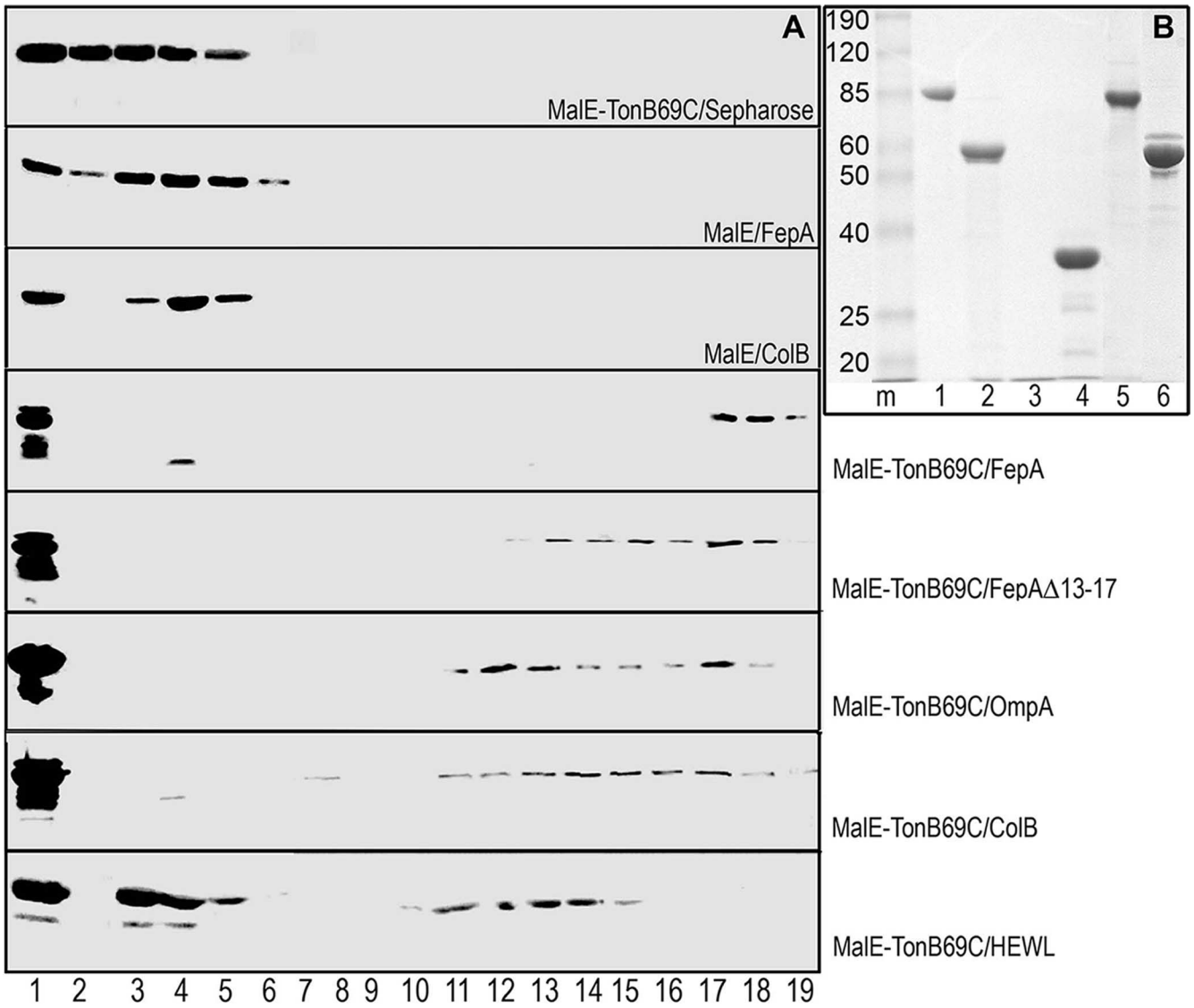

FIG. 3. Affinity chromatography of MalE-TonB69C on agarose modified with proteins. (A) Purified MalE and MalETonB69C were tested for their ability to adsorb to Sepharose 6B that was derivatized with individual purified proteins. The sections of panel A show different chromatographic experiments (labeled to the right with the test protein/immobilized protein). The top three sections are control experiments: MalE-TonB69C chromatographed on unmodified Sepharose 6B, and MalE chromatographed on Sepharose 6B modified with FepA or ColB. MalE did not adsorb to any of the modified agaroses; for brevity, only the results with FepA-Sepharose and ColB-Sepharose are shown. The remaining sections show MalE-TonB69C passed over Sepharose modified with the indicated proteins. In each experiment, the test protein starting material (MalE or MalE-TonB69C; lane 1) was loaded on the column, which was washed with 10 column volumes of TBS (pH 7.5) (lanes 2 to 7), followed by a linear salt gradient (0 to 0.5 M NaCl in TBS [pH 7.5]; lanes 8 to 19). Fractions (1 ml) were collected and resolved on SDS-polyacrylamide gels that were transferred to nitrocellulose and developed with mouse monoclonal anti-MalE serum (93). HEWL, hen egg white lysozyme. (B) Purified proteins. The SDS-polyacrylamide gel (stained with Coomassie blue) shows the purified proteins that were conjugated to Sepharose: FepA, ColB, hen egg white lysozyme, OmpA, FepAΔ13-17, in lanes 1 to 5, respectively, and purified MalE-TonB69C, which was passed over the modified agaroses (lane 6). The positions of molecular size markers (m) (in kilodaltons), the BenchMark prestained protein ladder (Invitrogen), are shown to the left of the gel.

degradation of both TonB and the GFP-TonB hybrid proteins, despite the inclusion of multiple protease inhibitors.

Both siderophore nutrition and colicin sensitivity assays showed, in contrast to the pTG constructs, that downstream localization of *tonB* from *ssgfp* in pGT and pGLT led to nearly wild-type activity of the TonB moiety (Fig. 6 and Table 3). Growth halos in nutrition tests were comparable in strains expressing wild-type TonB or the GFP-TonB fusion proteins, suggesting that the hybrid proteins facilitated siderophore uptake with an affinity and rate similar to those of wild-type TonB. ^{59}FeEnt uptake assays confirmed and clarified the wild-type activity of TonB in the hybrid proteins (Fig. 6; Table 3). The affinity for FeEnt of cells harboring pGT and pGLT was subnanomolar and statistically indistinguishable (dissociation constant [K_d] values of ≈0.4 nM) from that of a prototypic *E. coli* strain (BN1071) or *E. coli* OKN1/pT23. This equivalence

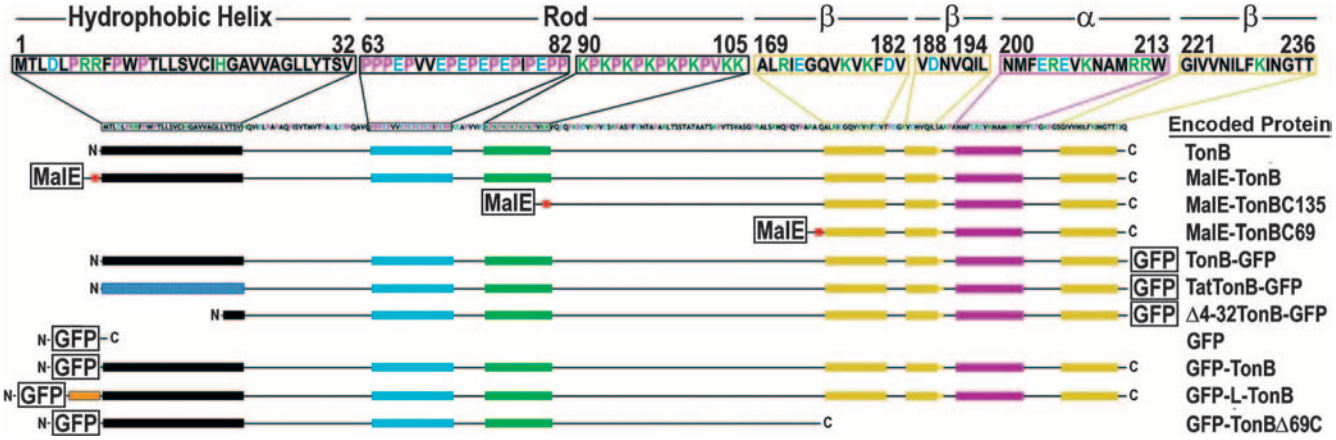

FIG. 4. MalE- and GFP-TonB fusion proteins. The illustration depicts some of the experimentally defined elements of TonB structure: the hydrophobic helix (residues 1 to 32; black rectangles in the schematic representations of fusion proteins shown below the sequence), the proline-rich rod domain (residues 63 to 105; cyan and green rectangles), and the C-terminal ββαβ domain (residues 169 to 236; yellow and magenta rectangles). Our constructions fused the complete *malE* or *ssgfp* structural genes to the *E. coli* K-12 *tonB* structural gene at different locations. We engineered MalE-TonB hybrid proteins that retained all the elements of TonB structure (MalE-TonB) or the rigid rod and the C terminus (MalE-TonBC135), or only the C-terminal ββαβ domain (MalE-TonBC69). We also designed constructs that encoded *ssgfp* downstream of wild-type *tonB* (TonB-GFP) and its derivatives with altered N termini (TatTonB-GFP and Δ4-32TonB-GFP). Last, we created plasmids that encoded *ssgfp* upstream of *tonB*, under the control of the *tonB* promoter, either alone (TonBp-GFP) or fused to wild-type TonB (GFP-TonB and GFP-L-TonB) or without the C-terminal ββαβ region (GFP-TonBΔ69C). The small red box denotes a designed factor Xa cleavage site, and the orange rectangle represents a designed, helical, 5-amino-acid linker region.

also appeared in the overall transport affinity for FeEnt, which was the same for all the strains (K_m values of ≈1 to 2 nM). The most noticeable difference between strain OKN1 harboring pT23, pGT, or pGLT was a 25% decrease in V_{max} in the latter two strains, which was consistent with their 25% lower FeEnt-binding capacity (Table 3). This reduction in FeEnt uptake rate accounts for the slightly larger growth halos in nutrition tests (3, 24). The decreased binding capacity translates into decreased V_{max}; the lower transport rate likely relates to slightly lower levels of GFP-TonB and GFP-L-TonB relative to that of TonB from pT23 (Fig. 5E and G). Still, the turnover numbers of FepA proteins in these strains were equivalent, indicating that the activities of GFP-TonB and GFP-L-TonB were indistinguishable from that of wild-type TonB itself. Thus, the presence of GFP at the N terminus of TonB had no measurable effect on the ability of the bacteria to transport iron.

Sequence relationship between TonB and YcsF. Analysis of the sequence of the TonB C terminus revealed homology to *E. coli ycfS*, which encodes a 320-amino-acid, proline-rich (8.4%) protein with a calculated mass of 34.6 kDa. YcfS is a member of a family of putative periplasmic proteins (7) of unknown function that contains a signal peptide (residues 1 to 23) followed by a hydrophobic, potential IM anchor, a lysin (LysM) motif (residues 45 to 91) that confers affinity for PG (7, 98), and a central proline-rich sequence. These attributes bear similarities to those of TonB, another proline-rich (16.7%) periplasmic protein that contains a hydrophobic N-terminal sequence, postulated to act as an IM anchor. CLUSTALW comparison of the *E. coli* LysM motif and the primary structure of TonB mapped a homologous region in the C terminus of TonB (residues 175 to 231; Fig. 7). Although the sequences of the 48-residue LysM motif and the C-terminal 69 amino acids of TonB are not highly conserved (19% identity, 77% homology), low overall identity is typical among LysM-containing, PG-binding cell envelope proteins (75, 98). In this alignment, it was noteworthy that D11 in LysM, at the center of the PG-binding surface (7), corresponded with E205, on the exterior surface of the TonB C terminus. Moreover, an LSQMAN comparison of the solved structure of the LysM motif from *E. coli* MltD (7) (RCSB 1e0g) and the C-domain of TonB (26) (RCSB 1Ihr) identified a second region of similarity on the external surface of TonB's dimeric ββαβ domain (Fig. 7). Superposition of the LysM crystal structure onto this second site revealed a nearly identical region of polypeptide folding in TonB. LSQMAN found 17 Cα positions (17 of 48; 35% of Cα) that aligned over 21 atoms with an overall root mean square deviation of 1.58 Å (Fig. 7). The most significant alignments of side chain residues were Arg 6, Arg 8, Asp 11, Lys 18, Arg 19, and His 20 on LysM, which superposed on Arg 171, Glu 173, Asp 189, Arg 211, Arg 212, and Trp 213, respectively, on TonB. In summary, the in silico analyses identified two regions in the TonB C terminus with an equivalent fold and aligned residues to LysM, suggesting that TonB has affinity for PG.

Binding of MalE-TonB69C to PG. To test this prediction, we purified sacculi from *E. coli* by SDS extraction and evaluated their ability to adsorb MalE-TonB69C. The purified PG fraction was free of cell envelope proteins, including the major proteins and iron-regulated LGP, as indicated by SDS-PAGE (Fig. 8) and by its transparency at 280 nm (data not shown). The purified sacculi precipitated MalE-TonB69C from solution, but not MalE nor FepB (Fig. 8). The binding reaction manifested saturation behavior: increasing amounts of PG bound and precipitated increasing amounts of MalE-TonB69C to a plateau value. The control proteins were themselves biologically active: maltose-binding protein was purified by amylose affinity columns, and chromatographically purified FepB (97) bound FeEnt (data not shown). Therefore, the affinity of

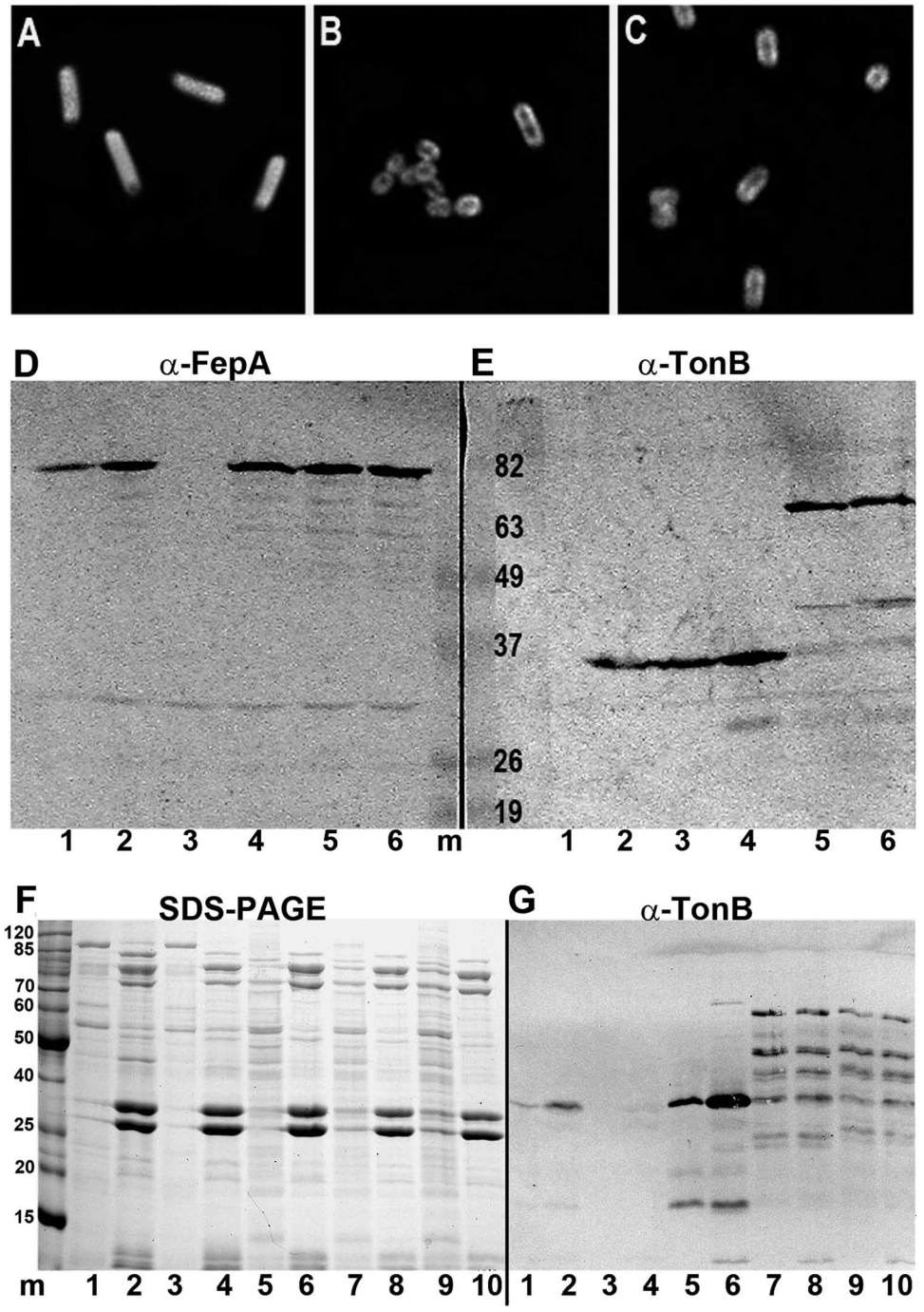

FIG. 5. (A to C) Fluorescence microscopic and electrophoretic analyses of GFP-TonB expression and localization. *E. coli* OKN3/pTpG (A), OKN3/pGT (B), and OKN3/pGLT (C) were grown in MOPS minimal medium and observed by fluorescence microscopy. Note that *E. coli* OKN3/pTpG, which expresses cytoplasmic GFP, showed diffuse, uniformly distributed fluorescence throughout the cells, whereas when GFP was fused upstream of TonB in *E. coli* OKN3/pGT and OKN3/pGLT, its fluorescence associated with the cell envelope, presumably from the association of TonB with the IM. (D and E) Expression of GFP-TonB hybrid proteins. A total of 10^8 cells of *E. coli* strains OKN1 (Δ*tonB*), BN1071 (*tonB*$^+$), OKN3 (Δ*fepA*), OKN1/pT23 (*tonB*$^+$), OKN1/pGT (*ssgfp-tonB*), and OKN1/pGLT (*ssgfp-L-tonB*), shown in lanes 1 to 6, respectively, were grown in MOPS minimal medium, lysed in sample buffer, and subjected to SDS-PAGE and Western immunoblotting with mouse anti-FepA monoclonal antibody 45 (α-FepA) (88) (D) or polyclonal rabbit anti-TonB (α-TonB) (E). The molecular size markers (m) (sizes in kilodaltons) were the BenchMark prestained protein ladder (Invitrogen). Panel D shows comparable expression of FepA in all *fepA*$^+$ strains; panel E shows the expression of wild-type TonB (lanes 2 to 4), GFP-TonB (lane 5), and GFP-L-TonB (lane 6) at comparable levels and the expected molecular sizes. (F and G) Fractionation of cell envelopes by French pressure cell lysis and sucrose gradient centrifugation. Bacteria were grown in MOPS minimal medium, collected by centrifugation, and lysed in a French pressure cell at 14,000 lb/in^2, and their membranes were resolved on sucrose step gradients and subjected to SDS-PAGE (F). IM samples from strains BN1071, OKN1, OKN1/pT23, OKN1/pGT, and OKN1/pGLT appear in lanes 1, 3, 5, 7, and 9, respectively; OM samples from the same strains appear in lanes 2, 4, 6, 8 and 10, respectively. In panel G, an identical gel was transferred to nitrocellulose and subjected to Western immunoblotting with rabbit anti-TonB sera.

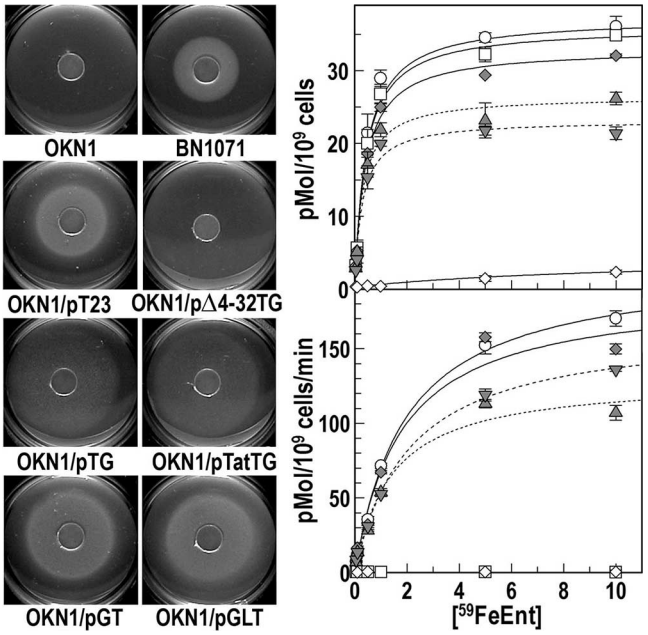

FIG. 6. FeEnt uptake by bacteria expressing GFP-TonB hybrid proteins. (Left) Siderophore nutrition tests showed the relative abilities of bacteria expressing hybrid TonB proteins to transport FeEnt (50 μM). When *ssgfp* was fused downstream of *tonB* (pTG and pTatTG), the function of FepA was compromised (large, faint growth halos); deletion of the TonB signal sequence (pΔ4-32TG) abrogated function. When GFP was fused upstream of TonB (pGT and pGLT), FeEnt uptake was comparable to that of strains expressing wild-type TonB (BN1071 and OKN1/pT23). Strain OKN3 (Δ*fepA*) gave the same result (data not shown) as the negative-control OKN1 (Δ*tonB*). (Right) The binding (top) and transport (bottom) abilities of strains expressing GFP-TonB and GFP-L-TonB were evaluated in ^{59}FeEnt uptake experiments. The binding and transport values are shown in picomoles/10^9 cells and in picomoles/10^9 cells/min, respectively. Strain OKN1 (□) harboring pT23 (◆), pGT (▲), or pGLT (▼) was compared to BN1071 (○) and its FepA-deficient derivative OKN3 (◇). GFP-TonB and GFP-L-TonB facilitated uptake with efficiencies similar to that of the wild-type TonB (see text for further explanation).

TonB for PG was not a general characteristic of periplasmic proteins, but a specific attribute of TonB itself.

DISCUSSION

The relationship between iron acquisition and microbial pathogenesis (1, 38, 51, 84, 104) underscores the importance of the role of TonB in cell envelope physiology. Passage of ferric complexes through the OM requires TonB activity, and one theory of this requirement is that TonB participates in transport energetics by capturing proton motive force from the IM (where its N terminus resides) and distributing it to the OM transporters (14, 23, 76, 82, 95). According to the "shuttle" model of TonB action, it associates with the IM proteins ExbB and ExbD (42, 56), acquires proton motive force-generated energy by an unknown structural transition, and transmits (15) or physically transports (55, 57) the energy across the periplasm to the OM. The proposed interaction of "energized" TonB with OM proteins entails recognition of ligand-bound receptors and release of the stored force to them by protein-protein interactions between the C-terminal residues of TonB and the TonB box sequence of the LGP (76, 95). The transferred energy presumably facilitates internalization of bound ferric siderophores and vitamin B_{12} (22), as well as bacterial susceptibility to B-group colicins and certain bacteriophages. Although the requirements for both energy and TonB in OM metal transport reactions are established, the participation of TonB in energy transduction or the bioenergetics of iron uptake remains undemonstrated.

Our experimental data relate to TonB function in several ways and suggest a model for its role in cell envelope biochemistry. We found that (i) TonB has a affinity for OM proteins, regardless of whether they contain a TonB box; (ii) GFP-TonB fusion proteins, which localize the hydrophilic GFP moiety in the cytoplasm, retain TonB function; and (iii) the C terminus of TonB binds PG, as a result of its comparable fold to the lysin structural motif.

It was unexpected that expression of MalE-TonB69C blocked FeEnt and ferrichrome uptake, but not colicin B kill-

TABLE 3. Binding and transport properties of selected strains

Strain/plasmid	Relevant genotype[a]	Nutrition test result[b]		ColB sensitivity[c]	Binding[d]		Transport[d]		
		FeEnt	Fc		K_d	Cap	K_m	V_{max}	k_8
BN1071	*fepA*$^+$ *tonB*$^+$	14	16	100	0.44	37.3	1.9	206	5.5
OKN3	Δ*fepA tonB*$^+$	0	16	R	NB	NB	NT	NT	NT
OKN1	*fepA*$^+$ Δ*tonB*	0	0	R	0.41	36	NT	NT	NT
OKN1/pT23	Δ*tonB*/*tonB*$^+$	15	16	100	0.4	33	1.8	188	5.7
OKN1/pGT	Δ*tonB*/*gfp*$^+$-*tonB*$^+$	16	17	100	0.31	26.5	1.4	130	4.9
OKN1/pGLT	Δ*tonB*/*gfp*$^+$-*L-tonB*$^+$	16	17	100	0.29	23.2	2.1	165	7.1

[a] For strain OKN1 carrying plasmid pGT or pGLT, the relevant genotype of the strain is shown before the slash, and the relevant genes for the plasmid are shown after the slash.

[b] Nutrition test results are expressed as the diameter of the growth halo around the disk (in millimeters) when the bacteria were supplied with FeEnt and ferrichrome (Fc) (Fig. 6).

[c] Colicin B (ColB) sensitivity was determined on LB plates and expressed relative to the susceptibility of strain BN1071. The strain was resistant (R) or as sensitive to colicin B as strain BN1071 was (shown as 100).

[d] K_d (nM), FeEnt-binding capacity (Cap) (pmol/10^9 cells), K_m (nM), and V_{max} (pmol/min/10^9 cells) were determined by GRAFIT 5.013 (Erithacus). The FepA-deficient strain OKN3 was simultaneously tested to determine nonspecific background levels of binding and transport (Fig. 6). NB, no binding; NT, no transport. For FeEnt-binding experiments, the mean standard errors for K_d and capacity were 17.4% and 6.2%, respectively. For FeEnt uptake experiments, the mean standard errors for K_m and V_{max} were 13.2% and 6.3%, respectively. The kinetic constant k_8 (3) shows turnover number: number of molecules/FepA protein/min. It was calculated by relating FeEnt transport rate to the amount bound: $k_8 = V_{max}$/capacity.

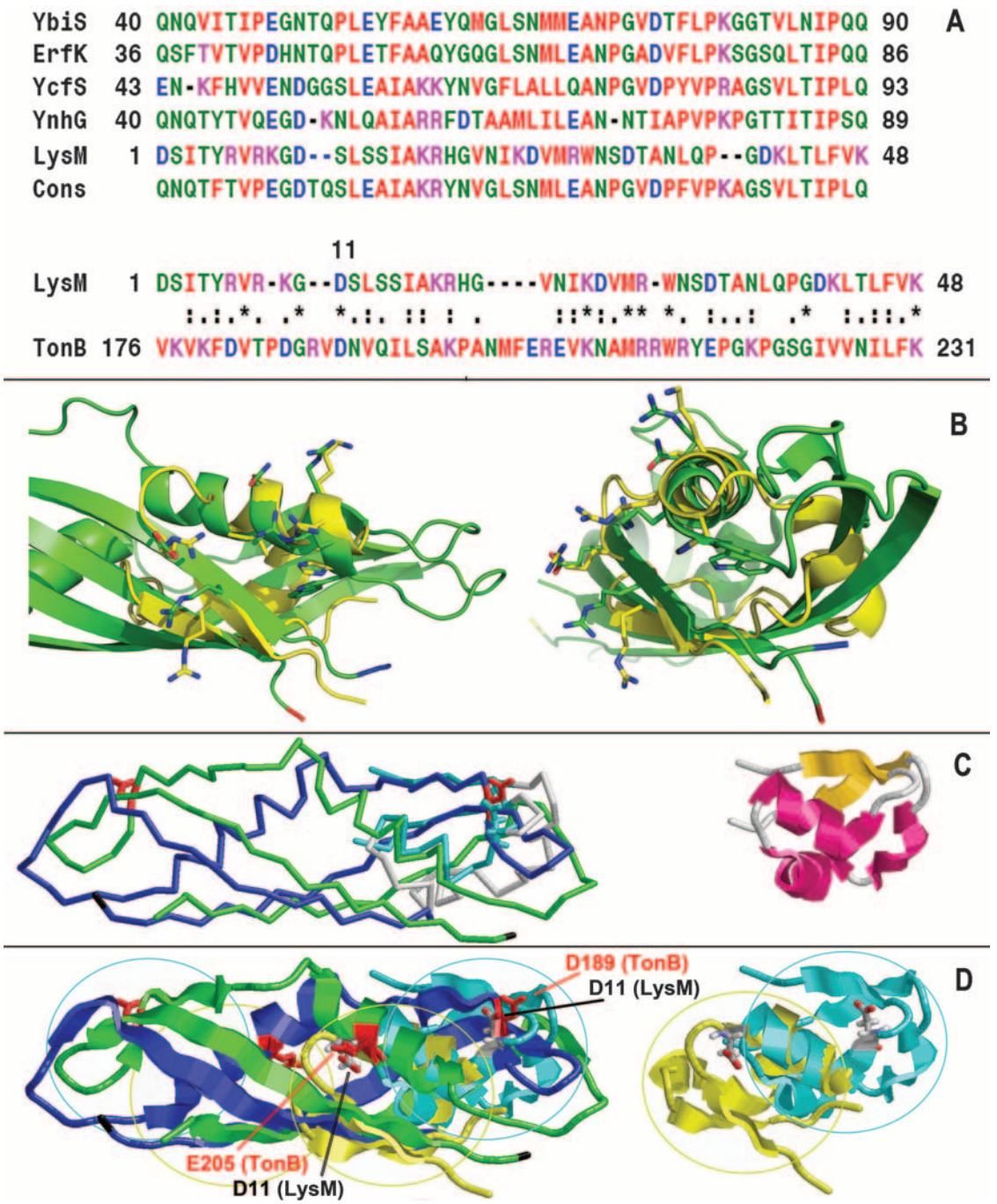

FIG. 7. Homology between the LysM domain and TonB. (A) CLUSTALW analysis of YcfS homologs. CLUSTALW was used to align the sequence of the LysM motif from the *E. coli* membrane-bound lytic murein transglycosylase D (MltD), which is structurally solved as an αβ domain (7), to the *E. coli* proteins YcfS, YbiS, YnhG, ErfK, and to the TonB C terminus. The figure shows the alignment of the relevant regions of the four proteins, and the consensus sequence (Cons) from the analysis. Hydrophilic residues are colored green, acidic residues are blue, basic residues are magenta, and hydrophobic residues are red. The consensus is also aligned to the sequence of the crystallized LysM domain of MltD. LysM alignment to TonB identified a sequence relationship at the C terminus of TonB. Asp 11 in LysM (red), which denotes the PG-binding surface in its structure (7), aligns with TonB residue Asp 189. (B) LSQMAN analysis of LysM and TonB. Using the crystallographic coordinates of LysM (7) and the TonB C terminus (26), LSQMAN found a second site of structural homology between the two polypeptides. The program identified a site in TonB (green), distinct from the region noted in panel A, to which LysM (yellow) superimposes. Nearly identical disposition and projection of residues occur in the two structures. The image on the right shows a 90° rotation of the image on the left. (C) On the left, the site identified by CLUSTALW in panel A was manually superimposed to the appropriate region of TonB structure, using α-carbon backbone representation. The regions of LysM that align with TonB (including D11 in stick format) are colored cyan; D189 in TonB, also in stick format, is colored red. The image on the right is a cartoon representation of LysM structure. (D) Four LysM motifs in the TonB dimer. Two LysM polypeptides were aligned to the right lobe of the dimeric TonB C-terminal domain (residues 165 to 239). The first (cyan polypeptide, cyan outline) was found by CLUSTALW; the second (yellow polypeptide, yellow outline) was found by LSQMAN; D11 (stick format, CPK color scheme) aligns with TonB residue D189 (stick format, red) in the first site and with E205 (stick format, red) in the second site. The reflection of these two sites in the left lobe of the structure (yellow and cyan outlines) creates four potential PG-binding sites in the TonB C-domain.

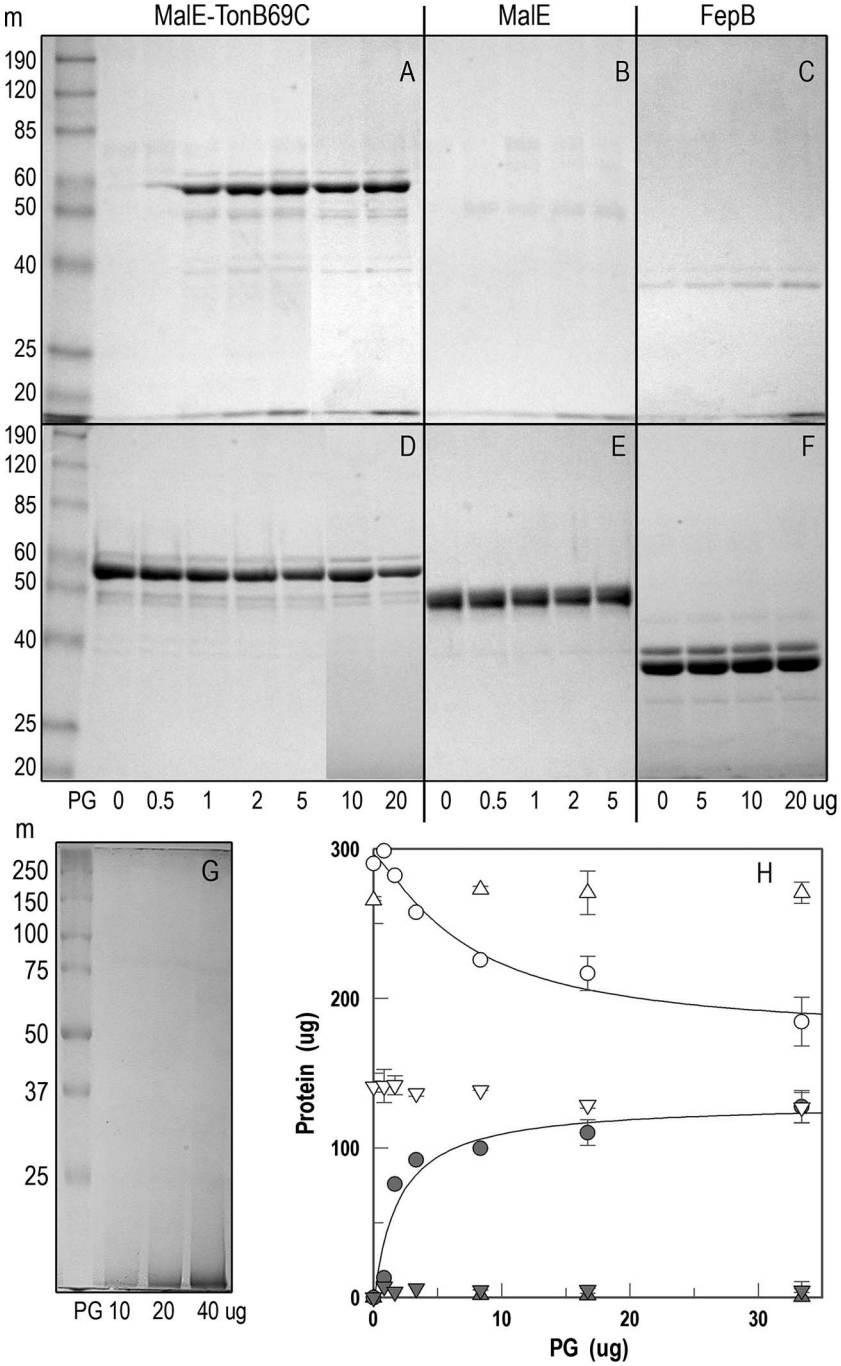

FIG. 8. Affinity of the TonB C terminus for PG. (A to F) Purified *E coli* PG was suspended in distilled water at 1.7 mg/ml. Increasing amounts of the PG solution were mixed with 30 μg of purified proteins MalETonB69C, MalE, and FepB in a final volume of 100 μl, incubated for 30 min at room temperature, and subjected to ultracentrifugation (100,000 × *g*, 45 min). The pellets (A to C) and supernatants (D to F) were resolved by SDS-PAGE, and the gels were stained with Coomassie blue. The positions of molecular size markers (m) (in kilodaltons), the BenchMark prestained protein ladder (Invitrogen), are shown to the left of the gels. Panels A and D are composite pictures from two separate experiments; the amount of added PG (in micrograms) is denoted beneath each lane. (G) SDS-PAGE of purified PG. Aliquots of the solution of purified sacculi were subjected to SDS-PAGE, and the gel was stained with Coomassie blue. The positions of molecular weight markers (m) (in kilodaltons), Precision Plus protein standards (Bio-Rad), are shown to the left of the gel. (H) Quantification of MalE-TonB69C precipitation in pellets and depletion from supernatants by PG. SDS-polyacrylamide gels were photographed, and the images were quantified using ImageQuant (Molecular Dynamics). Filled symbols are derived from analysis of pellets, while open symbols are derived from analysis of supernatants: MalE-TonB69C (circles) was precipitated, while MalE (inverted triangles) and FepB (triangles) were not precipitated by PG. The quantities of protein and PG (in micrograms) are shown on the *y* and *x* axes. The graph depicts the means ± standard errors (error bars) from two experiments.

ing. These data indicate that the ferric siderophores and the toxin diverge in their transport pathways at the stage inhibited by the isolated TonB C terminus. The inhibition of a TonB-dependent process by MalE-TonB69C in the periplasm demonstrated that the TonB C terminus folded properly in the chimeric protein, as was observed for other constructs that expressed it in the periplasm (43), and for TolA (12). Fluorescence spectra of the purified fusion protein concurred with this conclusion: W213 in TonB69C was preferentially quenched by acrylamide and quenched less by iodide and cesium, suggesting, as seen in crystal structures (26, 76, 95), that it localizes in a weakly polar environment (21, 102) where it is more accessible to the hydrophobic quencher than to the hydrated ions. The positive ion likely quenched most poorly as a result of repulsion from basic residues (arginines 187, 211, 212, and 214) in the proximity of W213, as seen in the crystal structure. Characterizations by CD were less definitive but reflected the presence of α and β structure. Quenching deviated from linearity at higher acrylamide concentrations, implying structural changes in the C terminus that result in noncollisional quenching effects. Together, the results suggested that in solution TonB69C assumed a biologically relevant tertiary structure: it folded into a globular domain with properties expected from the TonB crystal structure. Once purified, MalE-TonB69C adsorbed to TonB-dependent and -independent proteins, showing that besides its affinity for the TonB box of siderophore receptors, the TonB C terminus nonspecifically adsorbs to other proteins, including OmpA. This finding, which concurs with previous reports (41), is mechanistically important because of the abundance of OmpA in the OM ($\sim 10^5$ copies/cell) (92). The globular periplasmic domain of OmpA (99) may constitute another target for recruitment into the β-sheet within the C terminus of TonB, and it is known to exist in close proximity to FepA (94) in the OM bilayer. When viewed in light of IM localization of its N terminus, these data suggest that TonB may specifically or nonspecifically bridge the cell envelope by adsorbing to the periplasmic domains of TonB-dependent or TonB-independent OM proteins, respectively. Previous experiments support this notion: elimination of its terminal 8 residues did not impair TonB function, whereas deletion of the last 15 amino acids blocked activity (4). A truncated form of TonB lacking residues 174 to 239 did not cross-link to OM proteins or associate with the OM (57).

Letain and Postle (57) proposed that TonB shuttles between the membranes of the cell envelope during its facilitation of metal transport, and Larsen et al. (55) reiterated this mechanism. The fluorescent, biologically active GFP-TonB hybrid proteins (expressed from pGT and pGLT) are relevant to this idea, because the residence of their GFP moiety in the cytoplasm prohibits their transposition from IM to OM. We found, as did others (31, 61, 66), that GFP does not fluoresce in the periplasm. The fluorescence of GFP-TonB and GFP-L-TonB implies cytoplasmic localization of the upstream GFP moiety, and their biological activity indicates cell envelope localization of the downstream TonB protein. These results argue against the shuttle model. Letain and Postle (57) studied the partitioning of TonB between the IM and OM and cited their results as evidence that it may physically depart the IM and specifically associate with LGP in the OM. Yet, the separation of cell envelope fractions by any existing methodology is imperfect and incomplete. The French pressure cell lysis/sucrose gradient centrifugation method depends on brute-force separation of cell envelope components: a pressure differential explodes cells and presumably peels their IM and OM apart. In even the best experiments, the IM contains OM proteins because the latter traverse the former during biogenesis, and IM proteins contaminate the OM fraction, at least in part from the inefficiency of the membrane separation, and potentially from the architecture and physiology of the cell envelope (see below). Therefore, the observation of IM proteins in the OM fractions and vice versa is difficult to interpret in a mechanistic sense. Furthermore, other models may explain the cell envelope fractionation results. If TonB bridges the periplasm by virtue of its N terminus in the IM and its C terminus is associated with PG or OM proteins, then this structural organization alone accounts for its appearance in both fractions when the cell envelope pulls apart. The membranes are broken during the French pressure cell lysis procedure, and it is pertinent that neither the precise architecture of the periplasm nor the nature of its physical disruption (i.e., the fracture planes) are known. Finally, whereas the IM is a fluid mosaic bilayer, the outer lipopolysaccharide leaflet confers asymmetry and reduced fluidity to the OM, creating a quasifrozen state in the presence of divalent cations (73). In addition, OM proteins associate with the PG polymer (2, 59, 75, 87). In the absence of adhesions or continuities, it is conceivable that the IM and OM might efficiently separate during French pressure cell-mediated lysis, but if proteins or PG conjoin the two membranes in specialized regions, as was postulated (44, 54), observed (8, 63), and justified on the basis of Omp, PG, and lipopolysaccharide biosynthesis pathways (10, 47), then the isolation of pure OM and IM fractions is unlikely. Hence, immunoblot characterizations of fractionated cell envelopes are potentially ambiguous and subject to interpretation. Despite these reservations, the fusion of GFP upstream of TonB significantly decreased association with the OM without compromising TonB function. While wild-type TonB, whether chromosome or plasmid mediated, preferentially fractionated with the OM (three- to fourfold), both GFP-TonB and GFP-L-TonB distributed approximately equally, demonstrating that the GFP moiety enhanced association with the IM. The distribution was not absolute, in that the fusion protein was also seen in the OM fraction. The presence of GFP-TonB fusions in the OM fraction underscores the point that French pressure cell-mediated lysis does not preserve the normal distribution of proteins in the IM and OM. The upshot of these considerations is that characterizations of fractionated cell envelopes are fraught with uncertainty.

The potential flaws in such fractionation experiments suggest that in vivo evidence provides more accurate information about the localization of TonB or its various domains in the cell envelope. The extrinsic fluorophore labeling study of Larsen et al. (55) adopted such an approach, but it lacked a definitive control and structural information about the target, N-terminal domain of TonB. Its conclusions are subject to question in that (i) the experiments did not exclude the possibility that the Oregon green fluorophore penetrated the IM bilayer, and (ii) it is not known where the target residue L3C normally resides (in the IM bilayer or on its inner or outer surface). Therefore, although the authors concluded that the

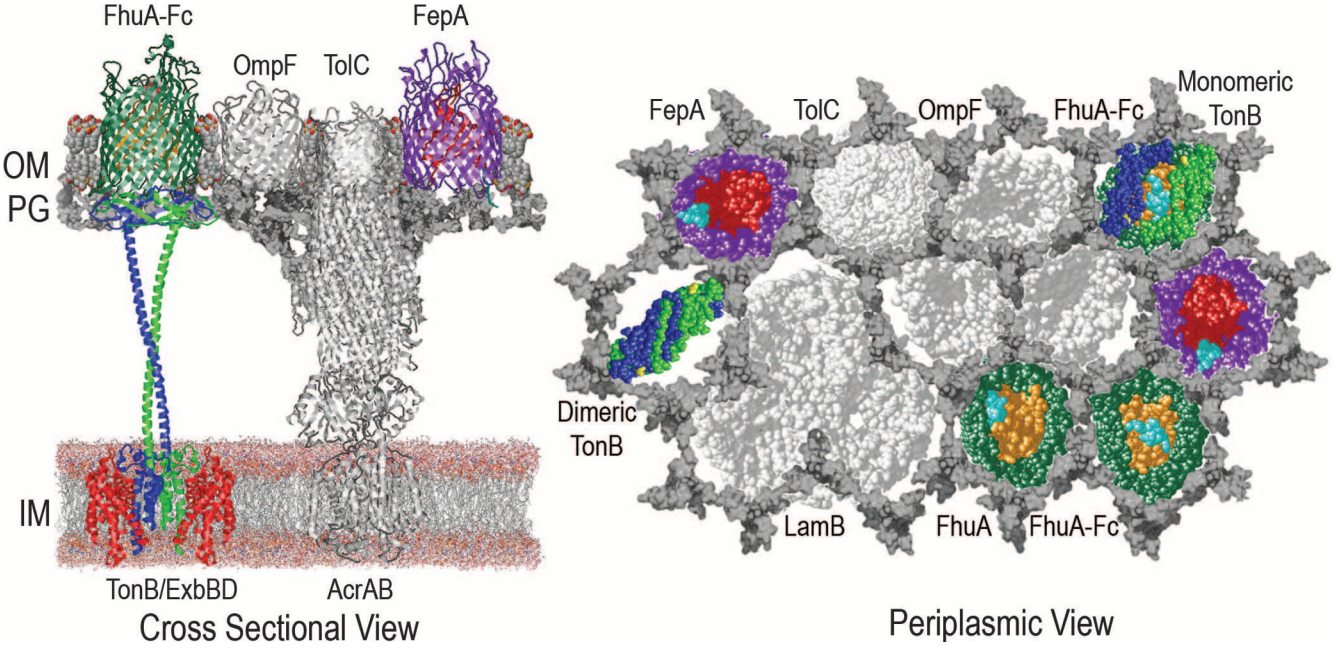

FIG. 9. PG-associated OM protein surveillance model of TonB action. (Left) In a cross-sectional view of the gram-negative bacterial cell envelope, dimeric TonB (green and blue) associates with the IM by α-helices in its N terminus that form a complex with ExbBD (red). TonB also contains extended lengths of rigid polypeptide (depicted here as coiled helices) that span the periplasm and LysM motifs in its C terminus that associate with the PG layer (gray) underlying the OM bilayer. The TonB dimer has general affinity for PG and TonB-independent OM proteins (e.g., OmpA), which tends to localize the C terminus at the periplasmic interface of the OM bilayer. The monomeric form of the C terminus, on the other hand, has a specific affinity for accessible TonB boxes of (ligand-bound) TonB-dependent receptors, resulting in their recruitment by its β-sheet. These dual affinities allow TonB to physically survey the periplasmic surface of the OM bilayer until it encounters bound LGP (FhuA [dark green and orange]). This motion across the internal surface of the OM may derive from movement of the N terminus in the fluid IM bilayer. FepA (purple and red) and the TonB-independent OM proteins OmpF (white) and TolC (white) are also shown associated with PG. The latter protein complexes with AcrAB in the IM bilayer, which provides a reference for the distance between the IM and OM bilayers. (Right) From a periplasmic view, the dimeric form of TonB (green and blue) moves among the roughly hexagonal, 50-Å cells of the PG polymer (gray), which associate with the β-barrels of OM proteins (TolC, OmpF, and LamB [all shown in white]). LGP in the OM bilayer may be ligand-free (FepA [purple β-barrel, red N-domain, and cyan TonB box]; FhuA [dark green β-barrel, orange N-domain, and cyan TonB box]) or ligand-bound (note FhuA at top and bottom right, with TonB box relocated to the center of the channel). The TonB-C-domain remains dimeric until it encounters a ligand-bound receptor (FhuA-Fc, top right) and then dissociates into a monomeric form that recruits the TonB box region into its β-sheet. This binding reaction and additional unknown energy-dependent reactions promote the unfolding of the LGP N-domain from the barrel and concomitant internalization of its bound metal complex. Crystallographic coordinates for the following proteins were from the RCSB Protein Data Bank (http://pdbbeta.rcsb.org/pdb/home/home.do): FepA (1FEP), FhuA (1BY3 and 1BY5), OmpF (1BT9), LamB (1MAL), TolC (1EK9), TonB C terminus (1IHR and 1QXX). The N-terminal and central regions of TonB and ExbBD were drawn (at this time, there are no high-resolution structural data for these polypeptides), and the PG polymer was drawn from Meroueh et al. (65).

TonB N terminus departed the IM bilayer in vivo, objections exist to this conclusion. The data that we report showing the fluorescence and functionality of GFP-TonB fusions undercut the shuttle model. The surface of *A. victoria* GFP contains 71 charged acidic or basic side chains, effectively precluding its movement through a membrane bilayer in vivo. Therefore, the transport ability of strains producing these fluorescent constructs demonstrates that TonB still functions when its N terminus remains anchored in the IM.

YcsF and its *E. coli* paralogs YnhG, YbiS, and ErfK form a family of cell envelope proteins. Each one, composed of approximately 320 amino acids, has an N-terminal hydrophobic region (putative transmembrane helix), a PG-binding domain (LysM) in the first third of primary structure, and a high percentage of proline residues (8 to 10%, roughly twice that of most proteins and half as much as TonB). The structural homology between the LysM motif and regions of the TonB C terminus raised the possibility of an affiliation between TonB and the murein sacculus. Experiments confirmed this inference: purified sacculi precipitated microgram quantities of purified MalE-TonB69C, but not MalE alone. Thus, in addition to its other binding functions, the TonB C-domain manifests significant affinity for PG. Although the in vivo disposition of TonB as a monomer or dimer remains uncertain, both may be physiologically rationalized, and there is experimental evidence for both the monomer in solution (78) and the dimer in live cells (90). However, LysM homology in TonB occurs only in the context of a dimeric C-domain, because the proposed binding clefts derive from α and β elements of different polypeptides; they do not involve the portion of the β-sheet that recruits heterologous polypeptides. The evidence that the LysM regions of TonB are suited for PG binding is strong. Its C-domain folds such that the backbone of region 2 has a root mean square deviation of 1.58 Å from that of LysM. Second, numerous residues relevant to binding are comparably distributed across the surfaces of both proteins (Fig. 7), including D189 and E205 in TonB, that project like D11, the residue that defines the PG-binding surface of LysM (7). The presence of

the lysin folds does not necessarily implicate them as responsible for the observed PG binding, and further experiments are warranted to confirm that conclusion. However, the lysin domains present potential PG-binding regions on the TonB C terminus; in the dimeric state, it contains four distinct sites that may interact with PG.

It is germane that the tripartite structural organization of TonB resembles the architecture of TolA, a component of the TolQRAB system that functions in maintenance of the structural integrity of the OM. The Tol system is required for infection by some bacteriophages (f1, M13, fd, and Ike) and group A colicins (E1, E2, E3, A, K, L, and N). Analogous to what we and others (43) found for the TonB C terminus, overexpression of the TolA C terminus in *tolA*$^+$ cells decreased TolA-dependent functions. These and other data illustrate the need for full-length TolA and TonB and the ability of their isolated C termini to interfere with OM transport systems. TolA spans the periplasm and associates with Pal in the OM by an interaction between two short sequences within the proteins (11, 79). Pal is a PG-binding lipoprotein that also contains the lysin motif. Finally, components of the Tol and Ton systems may substitute for each other, as illustrated by the complementation of *exbB* and *exbD* strains by homologous proteins of the Tol system, TolQ and TolR (16, 17). In summary, the homologous sequences and analogous results for the components of the TolA- and TonB-dependent transport systems imply similar mechanisms of action, which in both cases involve association with PG.

The persistent association of the N terminus of TonB with the IM and the general affinity of its C terminus for PG and OM proteins clarify the disposition of TonB in the cell envelope. Combined with a body of genetic, biochemical, and structural data, our results portray a cell envelope (Fig. 9) in which TonB normally spans the periplasm, temporarily or permanently adhering the IM and OM together at certain locations (i.e., adhesion zones [9, 54]). OM proteins may covalently or noncovalently associate with PG in vivo, including lipoprotein (19), Pal (75), OmpF (2, 59, 87), and FepA (data not shown). Neither OmpF nor FepA has periplasmic domains, so their association with PG must occur at the internal surface of the OM, and high-resolution microscopic studies show the PG polymer in contact with the OM bilayer (63). Recent structural data indicate that PG forms a honeycomb of 50-Å cells beneath the OM, creating a framework for association with OM proteins (65). The approximate 50-Å diameter of both OM β-barrels and the dimeric TonB C terminus, which are not likely coincidental, raise the possibility that the latter moves across the cells in this matrix until it encounters ligand-bound siderophore receptors. Bound LGP are distinguished by the repositioning of their TonB box to the center of their pores (33, 58), and in monomeric form, TonB may intercalate these polypeptides into its C-terminal βαβ domain (76, 95).

These points suggest a mechanism that we have designated "membrane surveillance," in which the interconvertible dimeric and monomeric forms of TonB display two distinct affinities. The nonspecific affinity of the dimeric C terminus for PG and TonB-independent OM proteins (e.g., OmpA) localizes it at the periplasmic interface of the OM bilayer. When it encounters a ligand-bound receptor, the affinity of the monomer for an accessible TonB box polypeptide supersedes the general affinity of the dimer, promoting dissociation and binding of the monomer to the LGP. This affiliation begins the process of ligand transport through the channel, which requires further energized reactions, and may occur by pulling, unfolding, or expelling the N terminus into the periplasm (60).

ACKNOWLEDGMENTS

The research was supported by NIH grant GM53836 and NSF grant MCB0417694 to P.E.K.

Thanks go to Amparo G. Marcos and Chuck Smallwood for their comments on the manuscript.

REFERENCES

1. **Abergel, R. J., M. K. Wilson, J. E. Arceneaux, T. M. Hoette, R. K. Strong, B. R. Byers, and K. N. Raymond.** 2006. Anthrax pathogen evades the mammalian immune system through stealth siderophore production. Proc. Natl. Acad. Sci. USA **103:**18499–18503.
2. **Alphen, W. V., and B. Lugtenberg.** 1977. Influence of osmolarity of the growth medium on the outer membrane protein pattern of *Escherichia coli*. J. Bacteriol. **131:**623–630.
3. **Annamalai, R., B. Jin, Z. Cao, S. M. Newton, and P. E. Klebba.** 2004. Recognition of ferric catecholates by FepA. J. Bacteriol. **186:**3578–3589.
4. **Anton, M., and K. J. Heller.** 1991. Functional analysis of a C-terminally altered TonB protein of *Escherichia coli*. Gene **105:**23–29.
5. **Arai, R., H. Ueda, A. Kitayama, N. Kamiya, and T. Nagamune.** 2001. Design of the linkers which effectively separate domains of a bifunctional fusion protein. Protein Eng. **14:**529–532.
6. **Axen, R., J. Porath, and S. Ernback.** 1967. Chemical coupling of peptides and proteins to polysaccharides by means of cyanogen halides. Nature **214:**1302–1304.
7. **Bateman, A., and M. Bycroft.** 2000. The structure of a LysM domain from *E. coli* membrane-bound lytic murein transglycosylase D (MltD). J. Mol. Biol. **299:**1113–1119.
8. **Bayer, M. E.** 1991. Zones of membrane adhesion in the cryofixed envelope of *Escherichia coli*. J. Struct. Biol. **107:**268–280.
9. **Bayer, M. H., W. Keck, and M. E. Bayer.** 1990. Localization of penicillin-binding protein 1b in *Escherichia coli*: immunoelectron microscopy and immunotransfer studies. J. Bacteriol. **172:**125–135.
10. **Bos, M. P., V. Robert, and J. Tommassen.** 2007. Biogenesis of the gram-negative bacterial outer membrane. Annu. Rev. Microbiol. **61:**191–214.
11. **Bouveret, E., R. Derouiche, A. Rigal, R. Lloubes, C. Lazdunski, and H. Benedetti.** 1995. Peptidoglycan-associated lipoprotein-TolB interaction. A possible key to explaining the formation of contact sites between the inner and outer membranes of *Escherichia coli*. J. Biol. Chem. **270:**11071–11077.
12. **Bouveret, E., L. Journet, A. Walburger, E. Cascales, H. Benedetti, and R. Lloubes.** 2002. Analysis of the *Escherichia coli* Tol-Pal and TonB systems by periplasmic production of Tol, TonB, colicin, or phage capsid soluble domains. Biochimie **84:**413–421.
13. **Bradbeer, C.** 1993. The proton motive force drives the outer membrane transport of cobalamin in *Escherichia coli*. J. Bacteriol. **175:**3146–3150.
14. **Braun, V.** 2006. Energy transfer between biological membranes. ACS Chem. Biol. **1:**352–354.
15. **Braun, V.** 1995. Energy-coupled transport and signal transduction through the gram-negative outer membrane via TonB-ExbB-ExbD-dependent receptor proteins. FEMS Microbiol. Rev. **16:**295–307.
16. **Braun, V.** 1989. The structurally related *exbB* and *tolQ* genes are interchangeable in conferring *tonB*-dependent colicin, bacteriophage, and albomycin sensitivity. J. Bacteriol. **171:**6387–6390.
17. **Braun, V., and C. Herrmann.** 1993. Evolutionary relationship of uptake systems for biopolymers in *Escherichia coli*: cross-complementation between the TonB-ExbB-ExbD and the TolA-TolQ-TolR proteins. Mol. Microbiol. **8:**261–268.
18. **Braun, V., and H. Wolff.** 1973. Characterization of the receptor protein for phage T5 and colicin M in the outer membrane of *E. coli* B. FEBS Lett. **34:**77–80.
19. **Braun, V., and H. Wolff.** 1970. The murein-lipoprotein linkage in the cell wall of *Escherichia coli*. Eur. J. Biochem. **14:**387–391.
20. **Brewer, S., M. Tolley, I. P. Trayer, G. C. Barr, C. J. Dorman, K. Hannavy, C. F. Higgins, J. S. Evans, B. A. Levine, and M. R. Wormald.** 1990. Structure and function of X-Pro dipeptide repeats in the TonB proteins of *Salmonella typhimurium* and *Escherichia coli*. J. Mol. Biol. **216:**883–895.
21. **Burstein, E. A., N. S. Vedenkina, and M. N. Ivkova.** 1973. Fluorescence and the location of tryptophan residues in protein molecules. Photochem. Photobiol. **18:**263–279.
22. **Cadieux, N., N. Barekzi, and C. Bradbeer.** 2007. Observations on the calcium dependence and reversibility of cobalamin transport across the outer membrane of *Escherichia coli*. J. Biol. Chem. **282:**34921–34928.
23. **Cadieux, N., P. G. Phan, D. S. Cafiso, and R. J. Kadner.** 2003. Differential

substrate-induced signaling through the TonB-dependent transporter BtuB. Proc. Natl. Acad. Sci. USA **100:**10688–10693.
24. **Cao, Z., Z. Qi, C. Sprencel, S. M. Newton, and P. E. Klebba.** 2000. Aromatic components of two ferric enterobactin binding sites in *Escherichia coli* fepA. Mol. Microbiol. **37:**1306–1317.
25. **Cao, Z., P. Warfel, S. M. Newton, and P. E. Klebba.** 2003. Spectroscopic observations of ferric enterobactin transport. J. Biol. Chem. **278:**1022–1028.
26. **Chang, C., A. Mooser, A. Pluckthun, and A. Wlodawer.** 2001. Crystal structure of the dimeric C-terminal domain of TonB reveals a novel fold. J. Biol. Chem. **276:**27535–27540.
27. **Chu, B. C., R. S. Peacock, and H. J. Vogel.** 2007. Bioinformatic analysis of the TonB protein family. Biometals **16:**16.
28. **Datsenko, K. A., and B. L. Wanner.** 2000. One-step inactivation of chromosomal genes in *Escherichia coli* K-12 using PCR products. Proc. Natl. Acad. Sci. USA **97:**6640–6645.
29. **di Guan, C., P. Li, P. D. Riggs, and H. Inouye.** 1988. Vectors that facilitate the expression and purification of foreign peptides in *Escherichia coli* by fusion to maltose-binding protein. Gene **67:**21–30.
30. **Evans, J. S., B. A. Levine, I. P. Trayer, C. J. Dorman, and C. F. Higgins.**1986. Sequence-imposed structural constraints in the TonB protein of *E. coli*. FEBS Lett. **208:**211–216.
31. **Feilmeier, B. J., G. Iseminger, D. Schroeder, H. Webber, and G. J. Phillips.** 2000. Green fluorescent protein functions as a reporter for protein localization in *Escherichia coli*. J. Bacteriol. **182:**4068–4076.
32. **Ferenci, T., and U. Klotz.** 1978. Affinity chromatographic isolation of the periplasmic maltose binding protein of *Escherichia coli*. FEBS Lett. **94:**213–217.
33. **Ferguson, A. D., E. Hofmann, J. W. Coulton, K. Diederichs, and W. Welte.** 1998. Siderophore-mediated iron transport: crystal structure of FhuA with bound lipopolysaccharide. Science **282:**2215–2220.
34. **Glauner, B.** 1988. Separation and quantification of muropeptides with high-performance liquid chromatography. Anal. Biochem. **172:**451–464.
35. **Glauner, B., J. V. Holtje, and U. Schwarz.** 1988. The composition of the murein of *Escherichia coli*. J. Biol. Chem. **263:**10088–10095.
36. **Gudmundsdottir, A., P. E. Bell, M. D. Lundrigan, C. Bradbeer, and R. J. Kadner.** 1989. Point mutations in a conserved region (TonB box) of *Escherichia coli* outer membrane protein BtuB affect vitamin B_{12} transport. J. Bacteriol. **171:**6526–6533.
37. **Guterman, S. K.** 1971. Inhibition of colicin B by enterochelin. Biochem. Biophys. Res. Commun. **44:**1149–1155.
38. **Hagan, E. C., and H. L. Mobley.** 2007. Uropathogenic *Escherichia coli* outer membrane antigens expressed during urinary tract infection. Infect. Immun. **75:**3941–3949.
39. **Hannavy, K., G. C. Barr, C. J. Dorman, J. Adamson, L. R. Mazengera, M. P. Gallagher, J. S. Evans, B. A. Levine, I. P. Trayer, and C. F. Higgins.** 1990. TonB protein of *Salmonella typhimurium*. A model for signal transduction between membranes. J. Mol. Biol. **216:**897–910.
40. **Hashimoto-Gotoh, T., F. C. Franklin, A. Nordheim, and K. N. Timmis.** 1981. Specific-purpose plasmid cloning vectors. I. Low copy number, temperature-sensitive, mobilization-defective pSC101-derived containment vectors. Gene **16:**227–235.
41. **Higgs, P. I., T. E. Letain, K. K. Merriam, N. S. Burke, H. Park, C. Kang, and K. Postle.** 2002. TonB interacts with nonreceptor proteins in the outer membrane of *Escherichia coli*. J. Bacteriol. **184:**1640–1648.
42. **Higgs, P. I., P. S. Myers, and K. Postle.** 1998. Interactions in the TonB-dependent energy transduction complex: ExbB and ExbD form homomultimers. J. Bacteriol. **180:**6031–6038.
43. **Howard, S. P., C. Herrmann, C. W. Stratilo, and V. Braun.** 2001. In vivo synthesis of the periplasmic domain of TonB inhibits transport through the FecA and FhuA iron siderophore transporters of *Escherichia coli*. J. Bacteriol. **183:**5885–5895.
44. **Ishidate, K., E. S. Creeger, J. Zrike, S. Deb, B. Glauner, T. J. MacAlister, and L. I. Rothfield.** 1986. Isolation of differentiated membrane domains from *Escherichia coli* and *Salmonella typhimurium*, including a fraction containing attachment sites between the inner and outer membranes and the murein skeleton of the cell envelope. J. Biol. Chem. **261:**428–443.
45. **Jesty, J., and M. P. Esnouf.** 1973. The preparation of activated factor X and its action on prothrombin. Biochem. J. **131:**791–799.
46. **Kadner, R. J.** 1990. Vitamin B12 transport in *Escherichia coli*: energy coupling between membranes. Mol. Microbiol. **4:**2027–2033.
47. **Kim, S., J. C. Malinverni, P. Sliz, T. J. Silhavy, S. C. Harrison, and D. Kahne.** 2007. Structure and function of an essential component of the outer membrane protein assembly machine. Science **317:**961–964.
48. **Klebba, P. E., M. A. McIntosh, and J. B. Neilands.** 1982. Kinetics of biosynthesis of iron-regulated membrane proteins in *Escherichia coli*. J. Bacteriol. **149:**880–888.
49. **Klebba, P. E., J. M. Rutz, J. Liu, and C. K. Murphy.** 1993. Mechanisms of TonB-catalyzed iron transport through the enteric bacterial cell envelope. J. Bioenerg. Biomembr. **25:**603–611.
50. **Kleywegt, G. J.** 1997. Detecting folding motifs and similarities in protein structure. Methods Enzymol. **277:**525–545.
51. **Koczura, R., and A. Kaznowski.** 2003. Occurrence of the *Yersinia* high-pathogenicity island and iron uptake systems in clinical isolates of *Klebsiella pneumoniae*. Microb. Pathog. **35:**197–202.
52. **Kodding, J., F. Killig, P. Polzer, S. P. Howard, K. Diederichs, and W. Welte.** 2005. Crystal structure of a 92-residue C-terminal fragment of TonB from *Escherichia coli* reveals significant conformational changes compared to structures of smaller TonB fragments. J. Biol. Chem. **280:**3022–3028.
53. **Kolodny, R., P. Koehl, and M. Levitt.** 2005. Comprehensive evaluation of protein structure alignment methods: scoring by geometric measures. J. Mol. Biol. **346:**1173–1188.
54. **Konisky, J.** 1979. Specific transport systems and receptors for colicins and phages. John Wiley and Sons, New York, NY.
55. **Larsen, R. A., T. E. Letain, and K. Postle.** 2003. In vivo evidence of TonB shuttling between the cytoplasmic and outer membrane in *Escherichia coli*. Mol. Microbiol. **49:**211–218.
56. **Larsen, R. A., M. G. Thomas, and K. Postle.** 1999. Proton motive force, ExbB and ligand-bound FepA drive conformational changes in TonB. Mol. Microbiol. **31:**1809–1824.
57. **Letain, T. E., and K. Postle.** 1997. TonB protein appears to transduce energy by shuttling between the cytoplasmic membrane and the outer membrane in *Escherichia coli*. Mol. Microbiol. **24:**271–283. (Erratum, **25:** 617.)
58. **Locher, K. P., B. Rees, R. Koebnik, A. Mitschler, L. Moulinier, J. P. Rosenbusch, and D. Moras.** 1998. Transmembrane signaling across the ligand-gated FhuA receptor: crystal structures of free and ferrichrome-bound states reveal allosteric changes. Cell **95:**771–778.
59. **Lugtenberg, B., R. Peters, H. Bernheimer, and W. Berendsen.** 1976. Influence of cultural conditions and mutations on the composition of the outer membrane proteins of *Escherichia coli*. Mol. Gen. Genet. **147:**251–262.
60. **Ma, L., W. Kaserer, R. Annamalai, D. C. Scott, B. Jin, X. Jiang, Q. Xiao, H. Maymani, L. M. Massis, L. C. Ferreira, S. M. Newton, and P. E. Klebba.** 2007. Evidence of ball-and-chain transport of ferric enterobactin through FepA. J. Biol. Chem. **282:**397–406.
61. **Ma, X., D. W. Ehrhardt, and W. Margolin.** 1996. Colocalization of cell division proteins FtsZ and FtsA to cytoskeletal structures in living *Escherichia coli* cells by using green fluorescent protein. Proc. Natl. Acad. Sci. USA **93:**12998–13003.
62. **March, S. C., I. Parikh, and P. Cuatrecasas.** 1974. A simplified method for cyanogen bromide activation of agarose for affinity chromatography. Anal. Biochem. **60:**149–152.
63. **Matias, V. R. F., A. Al-Amoudi, J. Dubochet, and T. J. Beveridge.** 2003. Cryo-transmission electron microscopy of frozen-hydrated sections of *Escherichia coli* and *Pseudomonas aeruginosa*. J. Bacteriol. **185:**6112–6118.
64. **Mengin-Lecreulx, D., and J. van Heijenoort.** 1985. Effect of growth conditions on peptidoglycan content and cytoplasmic steps of its biosynthesis in *Escherichia coli*. J. Bacteriol. **163:**208–212.
65. **Merouehe, S. O., K. Z. Bencze, D. Hesek, M. Lee, J. F. Fisher, T. L. Stemmler, and S. Mobashery.** 2006. Three-dimensional structure of the bacterial cell wall peptidoglycan. Proc. Natl. Acad. Sci. USA **103:**4404–4409.
66. **Mileykovskaya, E., Q. Sun, W. Margolin, and W. Dowhan.** 1998. Localization and function of early cell division proteins in filamentous *Escherichia coli* cells lacking phosphatidylethanolamine. J. Bacteriol. **180:**4252–4257.
67. **Miller, I., D. Maskell, C. Hormaeche, K. Johnson, D. Pickard, and G. Dougan.** 1989. Isolation of orally attenuated *Salmonella typhimurium* following Tn*phoA* mutagenesis. Infect. Immun. **57:**2758–2763.
68. **Miller, J. H.** 1972. Experiments in molecular genetics. Cold Spring Harbor Laboratory, Cold Spring Harbor, NY.
69. **Neidhardt, F. C., P. L. Bloch, and D. F. Smith.** 1974. Culture medium for enterobacteria. J. Bacteriol. **119:**736–747.
70. **Neilands, J. B., T. Peterson, and S. A. Leong.** 1980. High affinity iron transport in microorganisms. ACS Symp. Ser. **140:**263–278.
71. **Newton, S. M., J. D. Igo, D. C. Scott, and P. E. Klebba.** 1999. Effect of loop deletions on the binding and transport of ferric enterobactin by FepA. Mol. Microbiol. **32:**1153–1165.
72. **Nikaido, H., and E. Y. Rosenberg.** 1983. Porin channels in *Escherichia coli*: studies with liposomes reconstituted from purified proteins. J. Bacteriol. **153:**241–252.
73. **Nikaido, H., and M. Vaara.** 1985. Molecular basis of bacterial outer membrane permeability. Microbiol. Rev. **49:**1–32.
74. **Oudega, B., W. J. Oldenziel-Werner, P. Klaasen-Boor, A. Rezee, J. Glas, and F. K. de Graaf.** 1979. Purification and characterization of cloacin DF13 receptor from *Enterobacter cloacae* and its interaction with cloacin DF13 in vitro. J. Bacteriol. **138:**7–16.
75. **Parsons, L. M., F. Lin, and J. Orban.** 2006. Peptidoglycan recognition by Pal, an outer membrane lipoprotein. Biochemistry **45:**2122–2128.
76. **Pawelek, P. D., N. Croteau, C. Ng-Thow-Hing, C. M. Khursigara, N. Moiseeva, M. Allaire, and J. W. Coulton.** 2006. Structure of TonB in complex with FhuA, *E. coli* outer membrane receptor. Science **312:**1399–1402.
77. **Payne, M. A., J. D. Igo, Z. Cao, S. B. Foster, S. M. Newton, and P. E. Klebba.** 1997. Biphasic binding kinetics between FepA and its ligands. J. Biol. Chem. **272:**21950–21955.
78. **Peacock, R. S., A. M. Weljie, S. P. Howard, F. D. Price, and H. J. Vogel.**

2005. The solution structure of the C-terminal domain of TonB and interaction studies with TonB box peptides. J. Mol. Biol. **345:**1185–1197.
79. **Pommier, S., M. Gavioli, E. Cascales, and R. Lloubes.** 2005. Tol-dependent macromolecule import through the *Escherichia coli* cell envelope requires the presence of an exposed TolA binding motif. J. Bacteriol. **187:**7526–7534.
80. **Porath, J., R. Axen, and S. Ernback.** 1967. Chemical coupling of proteins to agarose. Nature **215:**1491–1492.
81. **Postle, K., and R. F. Good.** 1983. DNA sequence of the *Escherichia coli tonB* gene. Proc. Natl. Acad. Sci. USA **80:**5235–5239.
82. **Postle, K., and R. A. Larsen.** 2007. TonB-dependent energy transduction between outer and cytoplasmic membranes. Biometals **20:**453–465.
83. **Postle, K., and W. S. Reznikoff.** 1978. *Hin*dII and *Hin*dIII restriction maps of the *attϕ80-tonB-trp* region of the *Escherichia coli* genome, and location of the *tonB* gene. J. Bacteriol. **136:**1165–1173.
84. **Prentice, A. M., H. Ghattas, and S. E. Cox.** 2007. Host-pathogen interactions: can micronutrients tip the balance? J. Nutr. **137:**1334–1337.
85. **Pugsley, A. P., and P. Reeves.** 1977. Uptake of ferrienterochelin by *Escherichia coli*: energy-dependent stage of uptake. J. Bacteriol. **130:**26–36.
85a. **Rabsch, W., L. Ma, G. Wiley, F. Z. Najar, W. Kaserer, D. W. Schuerch, J. E. Klebba, B. A. Roe, J. A. Laverde-Gomez, M. Schallmey, S. M. Newton, and P. E. Klebba.** 2007. FepA- and TonB-dependent bacteriophage H8: receptor binding and genomic sequence. J. Bacteriol. **189:**5658–5674.
86. **Roof, S. K., J. D. Allard, K. P. Bertrand, and K. Postle.** 1991. Analysis of *Escherichia coli* TonB membrane topology by use of PhoA fusions. J. Bacteriol. **173:**5554–5557.
87. **Rosenbusch, J. P.** 1974. Characterization of the major envelope protein from *Escherichia coli*. Regular arrangement on the peptidoglycan and unusual dodecyl sulfate binding. J. Biol. Chem. **249:**8019–8029.
88. **Rutz, J. M., J. Liu, J. A. Lyons, J. Goranson, S. K. Armstrong, M. A. McIntosh, J. B. Feix, and P. E. Klebba.** 1992. Formation of a gated channel by a ligand-specific transport protein in the bacterial outer membrane. Science **258:**471–475.
89. **Saier, M. H., Jr.** 2000. Families of proteins forming transmembrane channels. J. Membr. Biol. **175:**165–180.
90. **Sauter, A., S. P. Howard, and V. Braun.** 2003. In vivo evidence for TonB dimerization. J. Bacteriol. **185:**5747–5754.
91. **Schnaitman, C. A.** 1973. Outer membrane proteins of *Escherichia coli*. I. Effect of preparative conditions on the migration of protein in polyacrylamide gels. Arch. Biochem. Biophys. **157:**541–552.
92. **Schweizer, M., H. Schwarz, I. Sonntag, and U. Henning.** 1976. Mutational change of membrane architecture. Mutants of *Escherichia coli* K12 missing major proteins of the outer cell envelope membrane. Biochim. Biophys. Acta **448:**474–491.
93. **Scott, D. C.** 2000. Ph.D. dissertation. University of Oklahoma, Norman.
94. **Scott, D. C., S. M. Newton, and P. E. Klebba.** 2002. Surface loop motion in FepA. J. Bacteriol. **184:**4906–4911.
95. **Shultis, D. D., M. D. Purdy, C. N. Banchs, and M. C. Wiener.** 2006. Outer membrane active transport: structure of the BtuB:TonB complex. Science **312:**1396–1399.
96. **Smit, J., Y. Kamio, and H. Nikaido.** 1975. Outer membrane of *Salmonella typhimurium*: chemical analysis and freeze-fracture studies with lipopolysaccharide mutants. J. Bacteriol. **124:**942–958.
97. **Sprencel, C., Z. Cao, Z. Qi, D. C. Scott, M. A. Montague, N. Ivanoff, J. Xu, K. M. Raymond, S. M. Newton, and P. E. Klebba.** 2000. Binding of ferric enterobactin by the *Escherichia coli* periplasmic protein FepB. J. Bacteriol. **182:**5359–5364.
98. **Steen, A., G. Buist, K. J. Leenhouts, M. El Khattabi, F. Grijpstra, A. L. Zomer, G. Venema, O. P. Kuipers, and J. Kok.** 2003. Cell wall attachment of a widely distributed peptidoglycan binding domain is hindered by cell wall constituents. J. Biol. Chem. **278:**23874–23881.
99. **Sugawara, E., M. Steiert, S. Rouhani, and H. Nikaido.** 1996. Secondary structure of the outer membrane proteins OmpA of *Escherichia coli* and OprF of *Pseudomonas aeruginosa*. J. Bacteriol. **178:**6067–6069.
100. **Szmelcman, S., J. M. Clement, M. Jehanno, O. Schwartz, L. Montagnier, and M. Hofnung.** 1990. Export and one-step purification from *Escherichia coli* of a MalE-CD4 hybrid protein that neutralizes HIV in vitro. J. Acquir. Immune Defic. Syndr. **3:**859–872.
101. **Vakharia, H. L., and K. Postle.** 2002. FepA with globular domain deletions lacks activity. J. Bacteriol. **184:**5508–5512.
102. **Vivian, J. T., and P. R. Callis.** 2001. Mechanisms of tryptophan fluorescence shifts in proteins. Biophys. J. **80:**2093–2109.
103. **Wayne, R., and J. B. Neilands.** 1975. Evidence for common binding sites for ferrichrome compounds and bacteriophage ϕ80 in the cell envelope of *Escherichia coli*. J. Bacteriol. **121:**497–503.
104. **Wyckoff, E. E., A. R. Mey, A. Leimbach, C. F. Fisher, and S. M. Payne.** 2006. Characterization of ferric and ferrous iron transport systems in *Vibrio cholerae*. J. Bacteriol. **188:**6515–6523.
105. **Yin, E. T., and S. Wessler.** 1968. Bovine thrombin and activated factor X. Separation and purification. J. Biol. Chem. **243:**112–117.